AIMS Mathematics, 10(9): 20412–20442.
DOI: 10.3934/math.2025912
Received: 03 June 2025
Revised: 21 August 2025
Accepted: 29 August 2025
Published: 05 September 2025

https://www.aimspress.com/journal/Math

Research article

Stochastic dynamics of influenza epidemic model with vaccination strategy

Shunping Ouyang, Guoqin Chen, Yue Xia, Guoxing Shi* and Yanbin Feng*

School of Mathematics and Computer Science, Yunnan Minzu University, Kunming 650500, China

* **Correspondence:** Email: sgx13608714737@163.com; 040269@ymu.edu.cn.

Abstract: A profound understanding of influenza transmission mechanisms is crucial for developing effective control strategies. This study first establishes a deterministic SAIV influenza model incorporating vaccination and asymptomatic carriers. The basic reproduction number R_0 is derived using the next-generation matrix method, followed by an analysis of equilibrium existence and stability. The existence of a transcritical bifurcation in the deterministic model is rigorously demonstrated through bifurcation theory. Subsequently, a stochastic SAIV model incorporating both white noise and Lévy jumps is formulated based on the deterministic framework. By employing Lyapunov function theory, the existence, uniqueness, and non-negative boundedness of the global positive solution are proven, ensuring biological plausibility. Furthermore, threshold conditions for disease extinction and persistence are analytically derived, providing a theoretical delineation of influenza fade-out or endemic transmission. Finally, model parameters are estimated using empirical influenza data, validating the accuracy of the deterministic model and the reliability of stochastic dynamical predictions. The results indicate that limited medical resources facilitate sustained transmission and reduce eradication probability, while environmental stochasticity further emphasizes the critical role of optimized resource allocation in influenza containment.

Keywords: influenza transmission; SAIV epidemic model; threshold dynamics; stochastic stability; resource optimization
Mathematics Subject Classification: 60G51, 34A09, 92D25

1. Introduction

Influenza is an acute respiratory infectious disease caused by influenza viruses of types A, B, and C. It is highly contagious, has a long history, and remains a major global public health concern. Globally, an estimated 3–5 million cases of severe illness and 250,000–500,000 deaths occur annually [1]. Transmission occurs via respiratory droplets from symptomatic and asymptomatic infected individuals, through close contact, and via fomites contaminated with the virus. Influenza is

characterized by a short incubation period and a high attack rate, predisposing populations to large-scale outbreaks [2]. Clinical manifestations vary depending on the viral strain, population characteristics, and individual health status [3]. Preventive measures primarily include vaccination, personal protective behaviors, and the use of antiviral agents.

Epidemiology [4] studies the outbreak patterns and dynamic behaviors of infectious diseases, analyzing the infection–immunity processes through theoretical methods and establishing disease transmission models. Analyzing the dynamic characteristics of these models helps predict whether a disease will dissipate or become localized. Due to the distinct transmission characteristics of infectious diseases, mathematical modeling is essential for understanding and managing their dynamics. It is also widely used in addressing complex problems in fields such as mathematical physics and engineering [5]. Numerous researchers have constructed models based on this premise to explore disease dynamics and optimize control strategies. For instance, Lee et al. [6] developed an age-structured optimal control model to optimize vaccination strategies. Bugalia et al. [7] proposed a delayed SEIR model, demonstrating that enhanced interventions could effectively reduce the transmission rate.

In practical implementation scenarios, infectious diseases are frequently subjected to stochastic perturbations. Such perturbations arise from a spectrum of factors, encompassing pathogen mutations, delays in vaccination campaigns, abrupt policy modifications, and seasonal climatic oscillations. In view of this, research investigating the impacts of environmental perturbations on disease transmission has attracted substantial scholarly interest [8, 9]. For example, Cao et al. [10] proposed a stochastic SIQR model with quarantine measures, proving the existence of a stationary distribution for disease persistence. Cai et al. [11] introduced nonlinear incidence rates and white noise disturbances to analyze the effect of R_0 on disease dynamics and established threshold conditions for disease extinction. Zhang et al. [12] combined deterministic and stochastic processes in an SIQS model to explore theoretical criteria for disease extinction and persistence under population fluctuations.

With the advancement of research, it has been revealed that the transmission of epidemics in real-world scenarios is impacted by a multitude of intricate factors. These include shortages of medical resources, emergent public health incidents, inadequate vaccine provision, environmental alterations, human-induced interventions, and uncontrolled population mobility. Such factors can elicit nonlinear responses and unpredictable variations within epidemiological systems, giving rise to critical consequences. Conventional models, which are predicated on stochastic differential equation models driven by noise, struggle to accurately forecast and characterize the actual dynamics of epidemic transmission [13]. Therefore, incorporating Lévy jump processes into infectious disease models has emerged as an effective solution [14]. Bao et al. [15] were the first to study a stochastic Lotka–Volterra population model with Lévy jumps, exploring its population dynamics.

Since then, Lévy jumps have been widely applied in infectious disease modeling. For instance, Yang et al. [16] discovered that Lévy jumps not only affect the epidemic threshold but also suppress outbreaks through high-intensity perturbations, providing new perspectives for control strategies against extreme public health events. Sabbar et al. [17] pointed out that Lévy noise is a core factor in the complexity of epidemic spread, supporting the optimization of control strategies under resource constraints. Kiouach et al. [18] investigated an SVIR model with perturbations from Brownian motion and Lévy jumps, highlighting that disease extinction and persistence are determined by multiple factors, including the intensity of white noise, the magnitude of Lévy jumps, and system parameters.

Although previous studies have explored the impact of perturbation factors on epidemic transmission, few models systematically integrate the limitations of healthcare resources, insufficient vaccination, and sudden environmental changes [19].

The application of Lévy jump processes in epidemic models has not been fully explored, and there is a lack of research focusing on the optimization of vaccination strategies and control measures under resource constraints. Particularly, in situations of strained healthcare resources and sudden events, the intensification of epidemic transmission and the potential disruption of vaccine and healthcare supplies remain critical issues that urgently need to be addressed [20, 21]. Therefore, this paper investigates the impact of constrained vaccine supply on infectious disease transmission, particularly under limited healthcare resources [22]. An SAIV model is constructed by incorporating nonlinear asymptomatic and symptomatic infectors to study its dynamic behavior. Furthermore, white noise and Lévy jump processes are introduced to simulate the effects of environmental disturbances and public health emergencies on epidemic transmission. The research aims to optimize vaccination strategies and emergency response measures, thereby enhancing the efficiency and sustainability of disease prevention and control.

The organization of this study is as follows: Section 2 presents the construction of the SAIV influenza model. Section 3 calculates the basic reproduction number and equilibria of the model, and discusses its stability. Section 4 extends the deterministic SAIV influenza model into a stochastic SAIV model by introducing white noise and Lévy noise and analyzes its dynamic behavior. Section 5 conducts numerical simulations to validate the applicability of the stochastic SAIV model. Section 6 summarizes the main conclusions.

2. Model formulation

In the study of influenza transmission dynamics, Wang et al. [23] proposed an A-type influenza model incorporating vaccination and asymptomatic infections. In this model, medical resources are assumed to be unlimited, and treatment efficiency is considered independent of the number of infected individuals. While this assumption may be reasonable for small-scale outbreaks, it fails to capture the saturation effect of healthcare resources during large-scale epidemics, thereby underestimating the epidemic peak and duration. Consequently, the model's predictive accuracy and its applicability in devising effective prevention and control strategies are substantially limited.

Studies have shown that the application of the saturated treatment term

$$h(X) = \frac{rX}{1 + \alpha X}$$

can more precisely depict the capacity bottleneck resulting from limited medical resources in large-scale epidemics and exert a significant impact on the disease transmission process [24, 25]. Building upon this idea, the present study extends the SAIV model proposed by Guan and Brauer et al. [23, 26] by incorporating a saturated treatment mechanism into the recovery processes of asymptomatic and symptomatic infected individuals. Specifically, the cure rates of different infection types under limited medical resources are described by

$$\frac{a_1 A}{1 + b_1 A} \text{ and } \frac{a_2 I}{1 + b_2 I}$$

respectively, thereby establishing the following model:

$$\begin{cases} \frac{dS}{dt} &= (1-p)\Lambda - \mu S - \varphi S - \beta S(I+\delta A) + \frac{a_1 A}{1+b_1 A} + \frac{a_2 I}{1+b_2 I} + \gamma_3 V, \\ \frac{dA}{dt} &= \delta\beta S A - \mu A - \nu A - \frac{a_1 A}{1+b_1 A}, \\ \frac{dI}{dt} &= \beta S I + \nu A - \mu I - \frac{a_2 I}{1+b_2 I}, \\ \frac{dV}{dt} &= p\Lambda + \varphi S - \mu V - \gamma_3 V, \end{cases} \tag{2.1}$$

where, S denotes the susceptible population, A represents asymptomatic infected individuals, I represents symptomatic infected individuals, and V denotes the vaccinated individuals. The total population is defined as $N = S + A + I + V$. Parameter definitions are provided in Table 1, and the schematic representation of the model is shown in Figure 1.

Table 1. Definitions of parameters in model (2.1).

Parameter	Definition	Source
Λ	The recruitment rate of the susceptible	[26]
p	Influenza immunization likelihood in the susceptible population	[26]
μ	The per capita natural mortality rate	[26]
φ	The vaccination rate of the susceptible	[26]
β	The transmission rate coefficient	[26]
δ	Transmission ability ratio between infectious diseases and vaccinated individuals	[26]
ν	The rate of the asymptomatic patient returning to the infectious	[26]
γ_3	The failure rate of vaccine	[26]
a_1	Highest efficacy in treating asymptomatic individuals	[24, 25]
a_2	The highest recovery rate among those who have contracted the infection	[24, 25]
b_1	Constraints on resources for managing patients without clinical symptoms	[24, 25]
b_2	Treatment capacity constraints for infected patients	[24, 25]

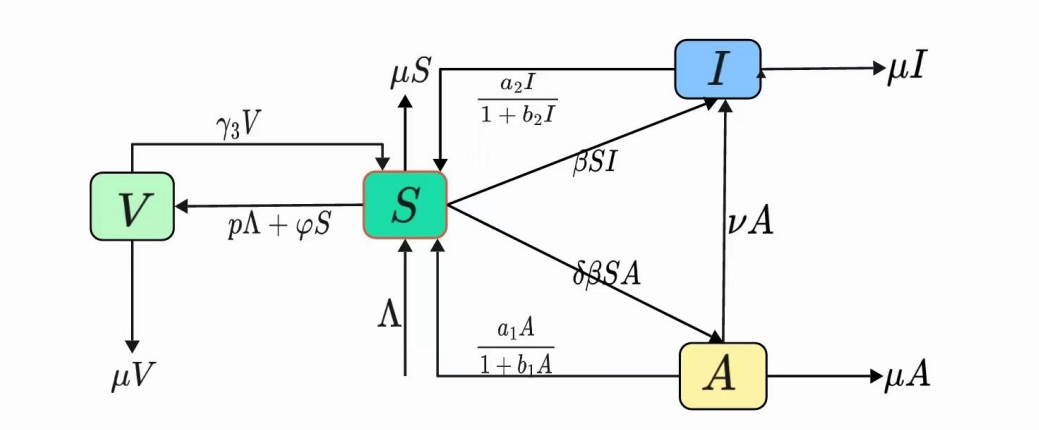

Figure 1. Schematic diagram of the SAIV epidemic transmission model (2.1).

3. Dynamic behavior of the ODE influenza epidemic model

The model (2.1) gives $N = S + A + I + V$, where $\frac{dN}{dt} = \Lambda - \mu N$ and $N(0) = \frac{\Lambda}{\mu}$. Thus, we conclude

$$N(t) = N(0)e^{-\mu t} + \Lambda \int_0^t e^{-\mu(t-s)}dt = N(0)e^{-\mu t} + \frac{\Lambda}{\mu}(1 - e^{-\mu t}) = \frac{\Lambda}{\mu},$$

this implies the existence of the global attractor for model (2.1) within

$$\mathcal{T} = \left\{(S, A, I, V) \in R_+^4 : S + A + I + V = \frac{\Lambda}{\mu}\right\}.$$

3.1. The basic reproduction number and Equilibria

The next-generation matrix method [27] will be applied to derive model (2.1)'s basic reproduction number. Let

$$\mathcal{F} = \begin{bmatrix} \delta\beta SA \\ \beta SI \end{bmatrix}, \mathcal{V} = \begin{bmatrix} \mu A + \nu A + \frac{a_1 A}{1+b_1 A} \\ -\nu A + \mu I + \frac{a_2 I}{1+b_2 I} \end{bmatrix}.$$

By calculation, we obtain

$$\begin{aligned} FV^{-1} &= \begin{bmatrix} \frac{\beta\Lambda(\mu-\mu p+\gamma_3)\delta}{\mu(\mu+\varphi+\gamma_3)} & 0 \\ 0 & \frac{\beta\Lambda(\mu-\mu p+\gamma_3)}{\mu(\mu+\varphi+\gamma_3)} \end{bmatrix} \begin{bmatrix} \mu+\nu+a_1 & 0 \\ -\nu & \mu+a_2 \end{bmatrix}^{-1} \\ &= \begin{bmatrix} \frac{\beta\Lambda(\mu-\mu p+\gamma_3)\delta}{\mu(\mu+\varphi+\gamma_3)(\mu+\nu+a_1)} & 0 \\ -\frac{\beta\Lambda(\mu p-\mu-\gamma_3)\nu}{\mu(\mu+\varphi+\gamma_3)(\mu+\nu+a_1)(\mu+a_2)} & \frac{\beta\Lambda(\mu-\mu p+\gamma_3)}{\mu(\mu+\varphi+\gamma_3)(\mu+a_2)} \end{bmatrix}. \end{aligned}$$

Thus, when $\delta > \frac{\mu+\nu+a_1}{\mu+\gamma_2}$ holds, the basic reproduction number for model (2.1) is given by

$$R_0 = \frac{\beta\Lambda\delta(\mu - \mu p + \gamma_3)}{\mu(\mu + \varphi + \gamma_3)(\mu + \nu + a_1)}.$$

The basic reproduction number R_0 is defined as the expected number of secondary infections produced by a single infectious individual over the course of their infectious period in a wholly susceptible population. When $R_0 < 1$, the infection will eventually die out; when $R_0 > 1$, sustained transmission and potential outbreaks may occur, although their realization is contingent on additional epidemiological factors. To further elucidate this relationship, numerical simulations were performed using the parameter estimates in Table 2 to quantify the effects of μ and γ_3 on R_0 (see Figure 2). Results indicate that increasing γ_3 elevates R_0, underscoring the importance of strengthening protective measures and reducing reinfection risk to suppress transmission. Conversely, higher ν is associated with a reduction in R_0. These findings imply that, to effectively mitigate influenza spread while maintaining a low natural mortality rate, public health strategies should prioritize reducing inter-regional mobility, minimizing contact between susceptible and infectious individuals, and implementing targeted, evidence-based interventions.

Table 2. Parameter values comparison for epidemic model.

Parameter	Value 1	Value 2	Source	Parameter	Value 1	Value 2	Source
p	0.159279	0.220495	Fitted	b_1	0.422645	0.463216	Fitted
Λ	20.00000	200.729291	Fitted	a_2	0.284990	0.916847	Fitted
μ	0.086798	0.000001	Fitted	b_2	0.001568	0.004707	Fitted
φ	0.074979	0.717417	Fitted	γ_3	0.003491	0.056851	Fitted
β	0.000327	0.000573	Fitted	$S(0)$	3000	3000	Assumed
δ	0.066475	0.390928	Fitted	$A(0)$	100	100	Assumed
ν	0.019223	0.163066	Fitted	$I(0)$	80	80	Assumed
a_1	0.009475	0.507182	Fitted	$V(0)$	70	70	Assumed

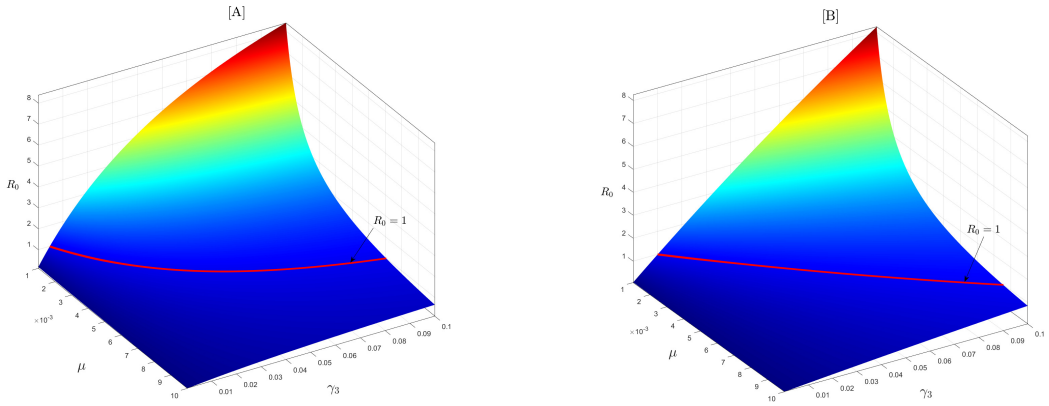

Figure 2. The impact of changes in parameters μ and γ_3 on R_0. The fixed parameters are respectively shown as value1 and value2 in Table 2.

The distinct non-disease equilibrium of the model given by model (2.1) is represented as $E_*(S_*, 0, 0, V_*)$, where

$$S_* = \frac{\Lambda[\mu(1-p)+\gamma_3]}{\mu(\mu+\varphi+\gamma_3)}, V_* = \frac{\Lambda(\mu p+\varphi)}{\mu(\mu+\varphi+\gamma_3)}.$$

The equilibrium $E^*(S^*, A^*, I^*, V^*)$ is defined as the endemic equilibrium of model (2.1), with its steady-state values obtained by solving the model under the condition $\frac{dS}{dt} = \frac{dA}{dt} = \frac{dI}{dt} = \frac{dV}{dt} = 0$, i.e.,

$$\begin{cases} (1-p)\Lambda - \mu S^* - \varphi S^* - \beta S^*(I^* + \delta A^*) + \frac{a_1 A^*}{1+b_1 A^*} + \frac{a_2 I^*}{1+b_2 I^*} + \gamma_3 V^* = 0, \\ \delta\beta S^* A^* - \mu A^* - \nu A^* - \frac{a_1 A^*}{(1+b_1 A^*)} = 0, \\ \beta S^* I^* + \nu A^* - \mu I^* - \frac{a_2 I^*}{(1+b_2 I^*)} = 0, \\ p\Lambda + \varphi S^* - \mu V^* - \gamma_3 V^* = 0. \end{cases} \tag{3.1}$$

When $A^* = 0$, the model (2.1) has an endemic equilibrium $E_0^*(S^*, 0, I^*, V^*)$, where

$$S^* = \frac{1}{\beta}\left(\mu + \frac{a_2}{\mu + b_2 I^*}\right), V^* = \frac{\varphi}{\beta(\mu+\gamma_3-p)}\left(\mu + \frac{a_2}{\mu + b_2 I^*}\right),$$

and $\frac{\Lambda}{\mu} = S^* + I^* + V^*$. Therefore, the infected population I^* can be derived from the following quadratic equation:

$$h_1(I^*) = c_1 I^{*2} + c_2 I^* + c_3 = 0, \tag{3.2}$$

where

$$c_1 = b_2 > 0, c_2 = \frac{(\varphi + \mu + \gamma_3 - p)b_2\mu}{\beta(\mu + \gamma_3 - p)} + \frac{b_2\mu - b_2\Lambda}{\mu}, c_3 = \frac{\beta\Lambda\delta(\mu - \mu p + \gamma_3)}{R_0\mu(\mu + \nu + a_2)} - \frac{\Lambda(\mu + \gamma_3 - p)\beta}{\mu(\mu + a_2 + b_2)} - p.$$

Assuming $c_3 = 0$ and $R_0 = 1$, β^* is given by

$$\beta^* = \frac{p\mu(\mu + \nu_3 + a_2)(\mu + a_2 + b_2) + \Lambda(\mu + \gamma_3 - p)}{\Lambda\delta(\mu - \mu p + \gamma_3)(\mu + a_2 + b_2) - \Lambda(\mu + \gamma_3 - p)}.$$

According to the fundamental properties of quadratic equations, if $\Lambda\delta(\mu - \mu p + \gamma_3)(\mu + a_2 + b_2) - \Lambda(\mu + \gamma_3 - p) > 0, c_2 > 0$, and $R_0 > 1$ (i.e., $\beta > \beta^*$), then Eq (3.2) admits a unique positive real root $I^* > 0$. This result establishes the existence of an endemic equilibrium $E_0^*(S^*, 0, I^*, V^*)$ for model (2.1). Conversely, if $R_0 \leqslant 1$ (i.e., $\beta < \beta^*$), Eq (3.2) admits no positive real root, thereby implying the nonexistence of an endemic equilibrium in model (2.1).

Additionally, when $A^* \neq 0$, from the second and fourth in Eq (3.1), we obtain

$$S^* = \frac{(\mu + \nu)(1 + b_1A^*) + a_1}{(1 + b_1A^*)\delta\beta}, V^* = \frac{(1 + b_1A^*)[p\Lambda\delta\beta + \varphi(\mu + \nu)] + \varphi a_1}{(1 + b_1A^*)\delta\beta(\mu + \gamma_3)}.$$

From the three equations in (3.1), it can be derived that

$$h_2(I^*) = m_1 I^{*2} + m_2 I^* + m_3 = 0, \tag{3.3}$$

where

$$m_1 = \beta S^* b_2 - \mu b_2 > 0, m_2 = \beta S^* + \nu b_2 A^* - \mu - a_2, m_3 = \nu A^* > 0,$$
$$\Delta = (\beta S^* + \nu A^* b_2 - \mu - a_2)^2 - 4(\beta S^* b_2 - \mu b_2)\nu A^*.$$

When $m_2 < 0$ and $\Delta = 0$, I^* can be derived from Eq (3.2) and is expressed as

$$I^* = \frac{\Lambda}{\mu} - S^* - V^* - A^* = \frac{\Lambda}{\mu} - \frac{P\Lambda\delta\beta + \varphi(\mu + \nu)}{\delta\beta(\mu + \gamma_3)} - \frac{\mu + \nu}{\delta\beta} - \frac{\varphi a_1 - a_1(\mu + \gamma_3)}{\delta\beta(1 + b_1A^*)(\mu + \gamma_3)} - A^*.$$

Subsequently, substituting A^* into Eq (3.3) yields

$$\begin{aligned}
h_3(A^*) = {} & b_1^3K_3A^{*5} + \left[(K_3 + C_3)b_1^2 - 2b_2^2K_3(K_1 - b_1) - \nu b_1^3 + \nu b_2 b_1^2\right]A^{*4} \\
& + \Big[(K_1 - b_1)^2 b_1K_3 - b_1^2K_3(K_1 - C_1) - 2b_1(K_1 - b_1)(K_3 + C_3) \\
& \quad + \nu b_1 b_2(K_1 - b_1) - b_1(b_1K_2 + \nu b_2) - 3b_1^2\nu\Big]A^{*3} \\
& + [b_1K_3(K_1 - b_1)(K_1 - C_1) - b_1(K_1 - C_1)(K_3 + C_3) + \nu b_1 b_2(K_1 - C_1) \\
& \quad - b_1(C_2 + K_2) + (b_1K_2 + \nu b_2)(K_1 - b_1) - 3b_1\nu]A^{*2} \\
& + \Big[b_1K_3(K_1 - C_1)^2 + (K_1 - b_1)(K_1 - C_1)(K_3 + C_3) + (b_1K_2 + \nu b_2)(K_1 - C_1) \\
& \quad + (C_2 + K_2)(K_1 - b_1) - \nu]A^* \\
& + (K_3 + C_3)(K_1 - C_1)^2 + (C_2 + K_2)(K_1 - C_1)
\end{aligned}$$

where

$$K_1 = \frac{\Lambda}{\mu} - \frac{P\Lambda\delta\beta + \varphi(\mu+\nu)}{\delta\beta(\mu+\gamma_3)} - \frac{\mu+\nu}{\delta\beta}, K_2 = \frac{(\mu+\nu)+a_1}{\delta} - \mu - a_2, K_3 = \frac{b_2(\mu+\nu)}{\delta} - \mu b_2,$$

$$C_1 = -\frac{\varphi a_1 - a_1(\mu+\gamma_3)}{\delta\beta(\mu+\gamma_3)}, C_2 = \frac{b_2 a_1}{\delta}, C_3 = \frac{b_2 a_1}{\delta}.$$

Under these conditions, A^* can be determined from $h_3(A^*)$. Therefore, when $m_2 < 0$ and $\Delta = 0$, the model (2.1) will have an epidemic equilibrium $E^*(S^*, A^*, I^*, V^*)$. To simplify the analysis, this study focuses on the case where a unique equilibrium exists. Specifically, when $R_0 > 1$, $\Delta = 0$ and $m_2 < 0$, model (2.1) admits a single endemic equilibrium, $E^* = (S^*, A^*, I^*, V^*)$, where the infected population is given by $I^* = -\frac{m_2}{2m_1}$. The Jacobian matrix of model (2.1) is

$$J = \begin{bmatrix} -\mu-\varphi-\beta(I+\delta A) & -\beta S\delta + \frac{a_1}{(1+b_1A)^2} & -\beta S + \frac{a_2}{(1+b_2I)^2} & \gamma_3 \\ \delta\beta A & \delta\beta S - \nu - \mu - \frac{a_1}{1+b_1A} + \frac{a_1 b_1 A}{(1+b_1A)^2} & 0 & 0 \\ \beta I & \nu & \beta S - \mu - \frac{a_2}{(1+b_2I)^2} & 0 \\ \varphi & 0 & 0 & -\mu-\gamma_3 \end{bmatrix},$$

and

$$det(J) = (\mu+\gamma_3)\mu e[(\beta S - \mu - f) - \beta I] + \delta\beta A[\nu(\beta S - f) + (\beta S - \nu - f)(g - \beta S\delta + e)] + \mu\varphi e(\beta S - \mu - f)$$

with

$$e = \frac{a_1 b_1 A}{(1+b_1A)^2}, f = \frac{a_2}{(1+b_2I)^2}, g = \frac{a_1}{(1+b_1A)^2}.$$

3.2. Equilibria stability

Lemma 3.1. *The disease-free equilibrium E_* is locally asymptotically stable when $R_0 < 1$, whereas it becomes unstable if $R_0 > 1$.*

Proof. The Jacobian matrix of model (2.1) evaluated at the disease-free equilibrium E_* is given by

$$J_{E_*} = \begin{bmatrix} -\mu-\varphi & \frac{\beta\delta\mu V_* - \beta\Lambda\delta + a_1\mu}{\mu} & \frac{\beta\mu V_* - \beta\Lambda + a_2\mu}{\mu} & \gamma_3 \\ 0 & \frac{-\beta\delta\mu V_* + \beta\Lambda\delta - \mu^2 - \nu\mu - \mu a_1}{\mu} & 0 & 0 \\ 0 & \nu & \frac{-\beta\mu V_* + \beta\Lambda - \mu^2 - \mu a_2}{\mu} & 0 \\ \varphi & 0 & 0 & -\mu-\gamma_3 \end{bmatrix}$$

and

$$det(J_{E_*}) = \frac{1}{\delta}(R_0 - 1)(\mu+\varphi)(\mu+\gamma_3)(\mu+\nu+a_1)[R_0(\mu+\nu+a_1) - \delta(\mu+a_2)] > 0. \tag{3.4}$$

By computation, the eigenvalues of the J_{E_*} are obtained as

$$\lambda_1 = -\mu < 0, \lambda_2 = -(\mu+\gamma_3+\varphi) < 0,$$
$$\lambda_3 = \frac{R_0(\mu+\nu+a_1) - \delta(\mu+a_2)}{\delta}, \lambda_4 = (R_0 - 1)(\mu+\nu+a_1).$$

Hence, if $R_0 < 1$ that is $\lambda_4 < 0$, E_* exhibits local asymptotic stability; conversely, when $R_0 > 1$, E_* becomes unstable. Verification is concluded. □

Next, we focus on the stability analysis of the endemic E^* of model (2.1), with particular attention to the case where $\Delta = 0$ and $m_2 < 0$. Drawing on the approach presented in [28], model (2.1) can be equivalently reformulated as

$$\begin{cases} A(t) = A(0)e^{-(\mu+\nu)t} + \delta\beta \int_0^t \mathcal{A}(t-s)A(s)S(s)ds - \int_0^t \mathcal{A}(t-s)\frac{a_1A(s)}{1+b_1A(s)}ds, \\ I(t) = I(0)e^{-\mu t} + \beta \int_0^t \mathcal{B}(t-s)I(s)S(s)ds + \nu \int_0^t \mathcal{B}(t-s)A(s)ds - \int_0^t \mathcal{B}(t-s)\frac{a_2I(s)}{1+b_2I(s)}ds, \\ V(t) = V(0)e^{-(\mu+\gamma_3)t} + P\Lambda \int_0^t C(t-s)ds + \varphi \int_0^t C(t-s)S(s)ds, \end{cases} \tag{3.5}$$

where

$$\mathcal{A}(t-s) = e^{-(\mu+\nu)(t-s)}, \mathcal{B}(t-s) = e^{-\mu(t-s)}, C(t-s) = e^{-(\mu+\gamma_3)(t-s)}.$$

For analytical tractability, we are applying the following translational transformation:

$$S(t) = \tilde{S}(t) + S^*, A(t) = \tilde{A}(t) + A^*, I(t) = \tilde{I}(t) + I^*, V(t) = \tilde{V}(t) + V^*,$$

the equilibrium E^* is shifted to the origin $(0, 0, 0, 0)$, where

$$S(t) = \frac{\Lambda}{\mu} - A(t) - I(t) - V(t) = S^* - \tilde{A}(t) - \tilde{I}(t) - \tilde{V}(t).$$

For brevity, we represent $\tilde{S}(t), \tilde{A}(t), \tilde{I}(t), \tilde{V}(t)$ as $S(t), A(t), I(t), V(t)$, where

$$\begin{aligned} A(t) = &-A^* + A(0)e^{-(\mu+\nu)t} + \delta\beta \int_0^t \mathcal{A}(t-s)S^*A^*ds - \int_0^t \mathcal{A}(t-s)\frac{a_1(A(s)+A^*)}{1+b_1(A(s)+A^*)}ds \\ &+\delta\beta \int_0^t \mathcal{A}(t-s)\{A(s)(S^* - A(s) - I(s) - V(s)) - A(s)[A(s) + I(s) + V(s)]\}ds, \end{aligned}$$

$$\begin{aligned} I(t) = &-I^* + I(0)e^{-\mu t} + \nu \int_0^t \mathcal{B}(t-s)A^*ds + \beta \int_0^t \mathcal{B}(t-s)I^*S^*ds + \nu \int_0^t \mathcal{B}(t-s)A(s)ds \\ &+\beta \int_0^t \mathcal{B}(t-s)I(s)(S^* - A(s) - I(s) - V(s) - I^*(A(s) + I(s) + V(s)))ds \\ &- \int_0^t \mathcal{B}(t-s)\frac{a_2(I(s)+I^*)}{1+b_2(I(s)+I^*)}ds, \end{aligned}$$

$$V(t) = -V^* + \frac{p\Lambda\varphi S^*}{\mu+\gamma_3} + (V(0) - \frac{p\Lambda\varphi S^*}{\mu+\gamma_3})e^{-(\mu+\gamma_3)t} - \varphi \int_0^t C(t-s)(A(s) + I(s) + V(s))ds.$$

As A^*, I^* and V^* satisfy the constraints below

$$A^* = \int_{-\infty}^{-t} \beta\delta A^*S^*\mathcal{A}(-\tau)d\tau, I^* = \int_{-\infty}^{-t} (\beta I^*S^* + \nu A^*)\mathcal{B}(-\tau)d\tau, V^* = \frac{p\Lambda\varphi S^*}{\mu+\gamma_3}.$$

Equation (3.5) admits the following equivalent representation

$$X(t) = F(t) + \int_0^t K(t-s)G(X(s))ds, \tag{3.6}$$

where

$$X(t) = \begin{bmatrix} A \\ I \\ V \end{bmatrix}, \quad F(t) = \begin{bmatrix} f_1(t) \\ f_2(t) \\ f_3(t) \end{bmatrix} = \begin{bmatrix} A(0)e^{-(\mu+\nu)t} - \int_{-\infty}^{-t} \beta\delta A^*S^*\mathcal{A}(-\tau)d\tau \\ I(0)e^{-\mu t} - \int_{-\infty}^{-t} (\beta I^*S^* + \nu A^*)\mathcal{B}(-\tau)d\tau \\ (V(0) - \frac{p\Lambda\varphi S^*}{\mu+\gamma_3})e^{-(\mu+\gamma_3)t} \end{bmatrix},$$

$$K(t) = \begin{bmatrix} \mathcal{A}(t) & 0 & 0 \\ 0 & \mathcal{B}(t) & 0 \\ 0 & 0 & C(t) \end{bmatrix}, \quad G(s) = \begin{bmatrix} G_1(s) \\ G_2(s) \\ G_3(s) \end{bmatrix},$$

$$\begin{aligned} G_1(X(s)) &= \beta\delta A(s)(S^* - A(s) - I(s) - V(s)) - \beta\delta A^*(A(s) + I(s) + V(s)) - \tfrac{a_1(A(s)+A^*)}{1+b_1(A(s)+A^*)}, \\ G_2(X(s)) &= \beta I(s)(S^* - A(s) - I(s) - V(s)) - \beta I^*(A(s) + I(s) + V(s)) + \nu A(s) - \tfrac{a_2(I(s)+I^*)}{1+b_2(I(s)+I^*)}, \\ G_3(X(s)) &= -\varphi(A(s) + I(s) + V(s)). \end{aligned}$$

Based on the above equivalent formulation, we establish the following lemma concerning the stability of the equilibrium $X_0 = (0, 0, 0)^T$ of model (3.6).

Lemma 3.2. *Let $X(t)$ be the solution of (3.6). If $F(t) \in C[0, \infty)$ with $F(t) \to 0$ as $n \to \infty$, and $K(t) \in L^1[0, \infty)$, then $X(t)$ remains nonnegative and bounded on $[0, \infty)$. Suppose $G(X) \in C^1(\mathbb{R}^2)$ with $G(0) = 0$, and the Jacobian of G at X_0 is nonsingular with all eigenvalues invertible. If*

$$\det\left(I - \int_0^\infty e^{-\lambda t} K(t)\mathcal{J}\, dt\right) = 0,$$

and all eigenvalues have negative real parts, then X_0 is locally asymptotically stable for (3.6).

Proof. The Jacobian of G at X_0 is

$$\mathcal{J} = \begin{bmatrix} \frac{(\delta\beta S^* - \delta\beta A^*)(1+b_1A^*)^2 - a_1}{(1+b_1A^*)^2} & -\delta\beta A^* & -\delta\beta A^* \\ -\beta I^* + \nu & \frac{(\beta S^* - \beta I^*)(1+b_2I^*)^2 - a_2}{(1+b_2I^*)^2} & -\beta I^* \\ -\varphi & -\varphi & -\varphi \end{bmatrix}$$

and $det(\mathcal{J}) = -\varphi(PQ + \delta\beta^2 A^* I^* + \delta\beta A^* Q + \beta I^* P) = -\varphi(\delta\beta A^* + P)(\beta I^* + Q) \neq 0$, where

$$P = \tfrac{(\delta\beta S^* - \delta\beta.A^*)(1+b_1A^*)^2 - a_1}{(1+b_1A^*)^2},\ Q = \tfrac{(\beta S^* - \beta I^*)(1+b_2I^*)^2 - a_2}{(1+b_2I^*)^2}.$$

Obviously, $\mathcal{J}$ is nonsingular.

Meanwhile,

$$\int_0^\infty e^{-(\lambda t)} K(t)\mathcal{J} dt = \begin{bmatrix} \frac{(\delta\beta S^* - \delta\beta A^*)(1+b_1A^*)^2 - a_1}{(\mu+\nu+\lambda)(1+b_1A^*)^2} & \frac{-\delta\beta A^*}{\mu+\nu+\lambda} & \frac{-\delta\beta A^*}{\mu+\nu+\lambda} \\ \frac{-\beta I^* + \nu}{\mu+\lambda} & \frac{(\beta S^* - \beta I^*)(1+b_2I^*)^2 - a_2}{(\mu+\lambda)(1+b_2I^*)^2} & \frac{-\beta I^*}{\mu+\lambda} \\ \frac{-\varphi}{\mu+\gamma_3+\lambda} & \frac{-\varphi}{\mu+\gamma_3+\lambda} & \frac{-\varphi}{\mu+\gamma_3+\lambda} \end{bmatrix},$$

and the corresponding characteristic equation is

$$det\left(Identity - \int_0^\infty e^{-\lambda t} K(t)\mathcal{J} dt\right) = \frac{w_3\lambda^3 + w_2\lambda^2 + w_1\lambda + w_0}{(\lambda + \mu + \nu)(\lambda + \mu)(\lambda + \mu + \gamma_3)w_3} = 0, \tag{3.7}$$

where

$$
\begin{aligned}
w_0 &= \{(\mu+\gamma_3+\varphi)[\mu(\mu+\nu)+\mu\delta\beta A^*+\delta(\beta S^*)^2] \\
&\quad +(\mu+\gamma_3)[\mu+\nu+\delta\nu A^* b_2-\delta(\beta S^*+\nu A^* b_2-\mu-a_2)]\beta I^*\}MN \\
&\quad +(\mu+\gamma_3)\beta(\delta A^* M a_2+I^* N a_1)+(\mu+\gamma_3+\varphi)a_1a_2>0. \\
w_1 &= \{(2\mu+\nu)(\mu+\gamma_3+\varphi)+\mu(\mu+\nu)+[(2\mu+\gamma_3+\varphi+\nu) \\
&\quad +\delta(2\mu+\gamma_3)+\delta\varphi][\nu A^* b_2-(\beta S^*+\nu A^* b_2-\mu-a_2)] \\
&\quad +(2\mu+\gamma_3+\nu)\beta I^*+[\delta(2\mu+\gamma_3)+\nu\delta]\beta A^* \\
&\quad +\delta\beta^2 S^*(S^*+A^*+I^*)\}MN+(\mu+a_2)Na_1 \\
&\quad +[(2\mu+\gamma_3+\varphi+\nu)+\delta\beta(A^*+S^*)]Ma_2 \\
&\quad +[(2\mu+\gamma_3+\varphi)+\beta I^*+\nu A^* b_2-(\beta S^*+\nu A^* b_2-\mu-a_2)]Na_1+a_1a_2>0, \\
w_2 &= [3\mu+\gamma_3+\nu+a_2+\varphi+\beta I^*+\delta\beta A^* \\
&\quad +(\nu A^* b_2-(\beta S^*+\nu A^* b_2-\mu-a_2))(1+\delta)]MN+a_2M+a_1N>0, \\
w_3 &= (1+b_1A^*)^2(1+b_2I^*)^2>0.
\end{aligned}
$$

Accordingly, under the condition $w_1w_2 - w_0w_3 > 0$, all characteristic roots of equation (3.7) possess strictly negative real parts, thereby ensuring that the equilibrium $X_0 = (0, 0, 0)$ of the dynamical model (3.6) is locally asymptotically stable. The proof is thus complete. □

By synthesizing the aforementioned analytical results and integrating the validated conclusions from References [29, 30], it is established that within the global attractor $\mathbf{\Gamma}$, the local asymptotic stability of the disease-free equilibrium E_* and the endemic equilibrium E^* can be extended to global asymptotic stability. Based on this, the following theorem is derived.

Theorem 3.1. *If $R_0 > 1$, $\Delta = 0$ and $m_2 < 0$, then the equilibrium E^* of model* (2.1) *is locally asymptotically stable.*

Theorem 3.2. *Let Γ denote the global basin of attraction for the disease dynamics. If $R_0 < 1$, the disease-free equilibrium E_* is globally asymptotically stable in Γ. Conversely, when $R_0 > 1$ and the additional conditions $\Delta = 0$ and $m_2 < 0$ are satisfied, the endemic equilibrium E^* is globally asymptotically stable in Γ.*

Theorem 3.3. *When $c_2 > 0$ and $A^* = 0$, the model (2.1) undergoes a transcritical bifurcation near the disease-free equilibriumE^* when $\beta = \beta^*$.*

Proof. When $\beta < \beta^*$, the model (2.1) has only one disease-free equilibrium E_*. When $\beta > \beta^*$ (i.e., $R_0 > 1$), the model has both a disease-free equilibrium E_* and an endemic equilibrium E_0^*. According to Theorem 3.2, when $R_0 < 1$, the disease-free equilibrium E_* of model (2.1) is globally asymptotically stable; however, when $R_0 > 1$, the endemic equilibrium E_0^* becomes unstable. For the endemic equilibrium E_0^*, when $\beta = \beta^*$, $I^* = 0$, and hence E_0^* coincides with the disease-free equilibrium E_*. When $\beta > \beta^*$, the endemic equilibrium E_0^* emerges. According to Theorem 3.2, when $\beta > \beta^*$, the endemic equilibrium E_0^* is globally asymptotically stable. Thus, the stability of model (2.1) undergoes a change near $\beta = \beta^*$. Based on reference [31], it can be inferred that model (2.1) undergoes a transcritical bifurcation at $\beta = \beta^*$. As illustrated in Figure 3[A], keeping other parameters constant and taking β as the bifurcation parameter, model (2.1) undergoes a transcritical bifurcation at $\beta = \beta^*$. Similarly, if γ_3 is selected as the bifurcation parameter, the model will also exhibit a transcritical bifurcation, as shown in Figure 3[A]. □

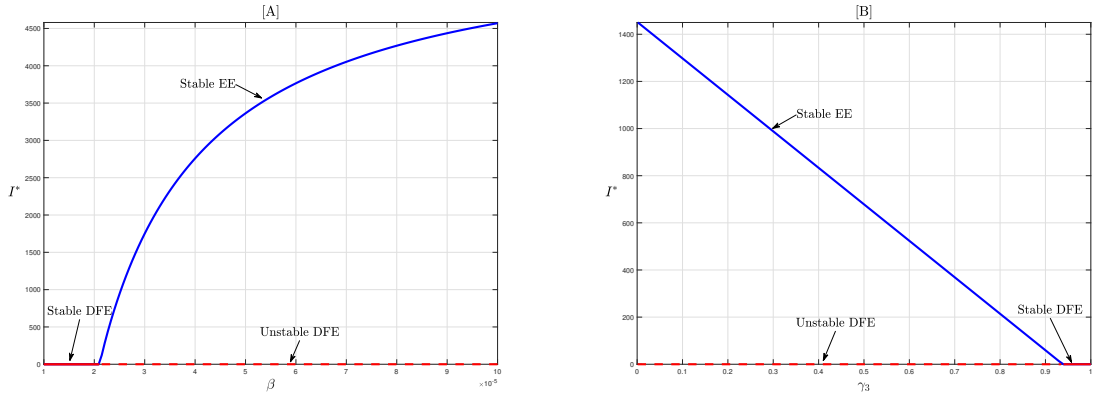

Figure 3. Transcritical bifurcation of model (2.1) with the bifurcation parameter β and γ_3. The parameters fixed as [A]: $\Lambda = 800, \gamma_3 = 0.2, \mu = 0.12, \varphi = 0.001, \delta = 0.00005, \nu = 0.016, a_1 = 0.006;, a_2 = 0.0012, b_1 = 0.09, b_2 = 0.004, p = 0.2$. [B]: $\Lambda = 500, \mu = 0.32, \varphi = 0.01, \beta = 0.003, \delta = 0.05, \nu = 0.026, a_1 = 0.36, a_2 = 0.001, b_1 = 0.03, b_2 = 0.05, p = 0.8$.

4. Dynamic behavior of the stochastic influenza epidemic model

In model (2.1), we investigate the dynamics of epidemic transmission under the constraint of limited medical resources. Under normal conditions, resource pressures such as insufficient ICU beds and shortages of medications prolong the viral shedding period, thereby increasing the risk of transmission [32–34]. However, when confronted with sudden events, such as extreme weather or disruptions in vaccine supply, the strain on the healthcare system intensifies sharply, further exacerbating the spread of the epidemic.

To simultaneously capture both continuous fluctuations and abrupt disruptive disturbances, we combine Gaussian white noise with a Lévy jump process driven by environmental factors; the former captures the regular stochastic fluctuations during the stable transmission phase of the disease, while the latter focuses on abrupt perturbations induced by extreme events. These two components act in synergy to authentically reconstruct the inherent randomness and uncertainty embedded in real-world transmission processes. Guided by this framework, thereby formulating the following model:

$$\begin{cases} dS &= [(1-p)\Lambda - \mu S - \varphi S - \beta S(I+\delta A) + \frac{a_1 A}{1+b_1 A} + \frac{a_2 I}{1+b_2 I} + \gamma_3 V]dt \\ &+ \delta_1 S\, dB_1(t) + \int_Y q_1(y) S(t-)\tilde{N}(dt,dy), \\ dA &= [\delta\beta S A - \mu A - \nu A - \frac{a_1 A}{1+b_1 A}]dt + \delta_2 A dB_2(t) + \int_Y q_2(y) A(t-)\tilde{N}(dt,dy), \\ dI &= [\beta S I + \nu A - \mu I - \frac{a_2 I}{1+b_2 I}]dt + \delta_3 I dB_3(t) + \int_Y q_3(y) I(t-)\tilde{N}(dt,dy), \\ dV &= [p\Lambda + \varphi S - \mu V - \gamma_3 V]dt + \delta_4 V dB_4(t) + \int_Y q_4(y) V(t-)\tilde{N}(dt,dy), \end{cases} \tag{4.1}$$

where the parameters in model (4.1) have the same meanings as those in model (2.1). Moreover,

- $S(t^-)$, $A(t^-)$, $I(t^-)$, and $V(t^-)$ denote the left-hand limits of $S(t)$, $A(t)$, $I(t)$, and $V(t)$, respectively.
- $B_i(t)$ $(i = 1, 2, 3, 4)$ denotes independent Brownian motions defined on the probability space

$(\Omega, F, \mathbb{P})$, with the filtration denoted by $\{F_t\}_{t\geq 0}$. For $i = 1, \ldots, 4$, $\sigma_i > 0$ represents the intensity of the Brownian motion.

- The term $q_i(y)$ $(i = 1, \ldots, 4)$ denotes the amplitude of the Lévy jump perturbations, with $q_i > -1$ to prevent excessive negative jumps that could cause drastic fluctuations in the system states.
- $N(dt, dy)$ denotes a Poisson random measure with characteristic measure λ, where λ is a finite measure supported on a measurable subset $\mathbb{Y} \subseteq (0, +\infty)$ (i.e., $\lambda(\mathbb{Y}) < +\infty$). Its compensated version is given by $\tilde{N}(dt, dy) = N(dt, dy) - \nu(dy)dt$, which is a martingale adapted to the filtration $\{F_t\}$.

Remark 4.1. *Assuming the Lévy noise is generated by a compound Poisson process, the corresponding Lévy measure $\nu(dy)$ is given by $\nu(dy) = \lambda F(dy)$, where $\lambda > 0$ represents the jump intensity, and $F(dy)$ denotes the probability distribution of the jump size Y, which is assumed to follow a zero-mean normal distribution, $N(0, \sigma^2)$. Under this assumption, the integral term $\int_Y [\ln(1 + q_i(y)) - q_i(y)]\nu(dy)$ can be computed analytically as $\lambda \cdot \mathbb{E}[\ln(1+q_iY)-q_iY]$. This formulation establishes a connection between the Lévy measure and physically meaningful distribution parameters, such as the frequency and intensity of impulsive events, thereby enhancing both the interpretability and practical applicability of the model.*

4.1. Existence and uniqueness of the global positive solution

In the analysis of the dynamics of epidemic models, the global existence, non-negativity, and boundedness of model solutions are of crucial importance. Herein, we employ the Lyapunov analysis method to prove the non-negativity and global existence of solutions for model (4.1) [35]. The state variables $S(t)$, $A(t)$, $I(t)$, and $V(t)$ must take positive values. Accordingly, we define

$$\Gamma = \left\{ (S(t), A(t), I(t), V(t)) \in \mathbb{R}^4_+ : S(t) + A(t) + I(t) + V(t) \leqslant \frac{\Lambda}{\mu} \right\}.$$

Lemma 4.1. *If $(S(0), A(0), I(0), V(0)) \in \Gamma$, then $(S(t), A(t), I(t), V(t)) \in \Gamma$ for all $t \geq 0$. That is, the set Γ is positively invariant under the dynamics of model* (4.1).

Proof. Let $(S(0), A(0), I(0), V(0)) \in \Gamma$, choose a sufficiently large positive integer n_0 such that each component of $(S(0), A(0), I(0), V(0))$ lies within the prescribed bounds. For every integer $n \geq n_0$, the terminal point is defined as

$$\tilde{\pi}_n = \inf \left\{ t > 0 : (S(t), A(t), I(t), V(t)) = X(t) \in \Gamma, X(t) \notin \left(\frac{1}{n}, \frac{\Lambda}{\mu} \right]^4 \right\},$$

$$\tilde{\pi} = \inf\{t > 0 : X(t) \notin \Gamma\}.$$

In fact, we need to show that for all $t > 0$, $\mathbb{P}(\tilde{\pi} < t) = 0$. Clearly, $\mathbb{P}(\tilde{\pi} < t) \leq \mathbb{P}(\tilde{\pi}_n < t)$. Next, we proceed with the proof as

$$\lim_{n\to+\infty} \sup \mathbb{P}(\tilde{\pi}_n < t) = 0.$$

Construct a C^4-function $F : \mathbb{R}^4_+ \to \mathbb{R}_+$, as

$$F(X) = \frac{1}{S} + \frac{1}{A} + \frac{1}{I} + \frac{1}{V}.$$

By applying Itô's formula [36], we obtain

$$\begin{aligned} dF(S,A,I,V) = \; & LF(S,A,I,V)dt - \tfrac{\delta_1}{S}dB_1(t) - \tfrac{\delta_2}{A}dB_2(t) - \tfrac{\delta_3}{I}dB_3(t) - \tfrac{\delta_4}{V}dB_4(t) \\ & - \int_Y \left[\tfrac{q_1(y)}{S+q_1(y)S} + \tfrac{q_2(y)}{A+q_2(y)A} + \tfrac{q_3(y)}{I+q_3(y)I} + \tfrac{q_4(y)}{V+q_4(y)V}\right]\tilde{N}(dt,dy). \end{aligned}$$

Therefore,

$$\begin{aligned} dF(S,A,I,V) \leqslant \; & \eta F(X)dt - \tfrac{\delta_1}{S}dB_1(t) - \tfrac{\delta_2}{A}dB_2(t) - \tfrac{\delta_3}{I}dB_3(t) - \tfrac{\delta_4}{V}dB_4(t) \\ & - \int_Y \left[\tfrac{q_1(y)}{S+q_1(y)S} + \tfrac{q_2(y)}{A+q_2(y)A} + \tfrac{q_3(y)}{I+q_3(y)I} + \tfrac{q_4(y)}{V+q_4(y)V}\right]\tilde{N}(dt,dy), \end{aligned} \tag{4.2}$$

where

$$\begin{aligned} \eta = \max\{ & \mu + \varphi + \beta(I+\delta A) + \delta_1^2 + \textstyle\int_Y \frac{q_1^2(y)}{1+q_1(y)}\nu(dy), \mu + \nu + a_1 + \delta_2^2 + \int_Y \frac{q_2^2(y)}{1+q_2(y)}\nu(dy), \\ & \mu + a_2 + \delta_3^2 + \textstyle\int_Y \frac{q_3^2(y)}{1+q_3(y)}\nu(dy), \mu + \gamma_3 + \delta_4^2 + \int_Y \frac{q_4^2(y)}{1+q_4(y)}\nu(dy)\}. \end{aligned}$$

By Fubini's Theorem [37], integrating inequality (4.2) and taking expectations yields

$$\mathbb{E}F(X(s)) \leqslant F(X(0)) + \eta \int_0^s \mathbb{E}F(X(\xi))d\xi.$$

Subsequently, by applying Gronwall's Lemma [38], we obtain $\mathbb{E}F(X(s)) \leqslant F(X(0))e^{\eta s}, \forall s \in [0, t \wedge \tilde{\pi}_n]$ and

$$\mathbb{E}F(X(t \wedge \tilde{\pi}_n)) \leqslant F(X(0))e^{\eta(t\wedge\tilde{\pi}_n)} \leqslant F(X(0))e^{\eta t}, \forall t \geq 0. \tag{4.3}$$

We consider that the components of $X(\tilde{\pi}_n)$ will not exceed $1/n$, given that $F(X(t \wedge \tilde{\pi}_n)) > 0$, we have

$$\mathbb{E}F(X(t \wedge \tilde{\pi}_n)) \geqslant \mathbb{E}\left[F(X(\tilde{\pi}_n))1_{\{\tilde{\pi}_n<t\}}\right] \geqslant n\mathbb{P}\left(\tilde{\pi}_n < t\right). \tag{4.4}$$

From (4.3) and (4.4), yields

$$\mathbb{P}\left(\tilde{\pi}_n < t\right) \leqslant \tfrac{F(X(0))e^{\eta t}}{n}, \forall t \geq 0.$$

Therefore,

$$\lim_{n\to+\infty} \sup \mathbb{P}(\tilde{\pi}_n < t) = 0.$$

That is, $\mathbb{P}(\tilde{\pi}_n = \infty) = 1$, which implies the existence of a solution.

From $\mathbb{P}(\tilde{\pi} < t) \leqslant \mathbb{P}(\tilde{\pi}_n < t)$, it follows directly that $\mathbb{P}(\tilde{\pi} < t) = 0$, and hence $\mathbb{P}(\tilde{\pi}_n = \infty) = 1$. For model (2.1), $N(t) = S(t) + A(t) + I(t) + V(t)$, which satisfies $\frac{dN}{dt} = \Lambda - \mu N$. Solving this equation yields the upper bound $\frac{\Lambda}{\mu}$, i.e., $N(t) = S(t) + A(t) + I(t) + V(t) \leq \frac{\Lambda}{\mu}$, which immediately implies that the region Γ is bounded. By the definition of an invariant set, since any trajectory with an initial condition in Γ remains within Γ and preserves positivity for all time, the set Γ is positively invariant with respect to model (4.1). □

Theorem 4.1. *For all initial conditions* $(S(0), A(0), I(0), V(0)) \in \mathbb{R}^4_+$, *the model* (4.1) *guarantees a solitary, globally positive solution* $(S(t), A(t), I(t), V(t)) \in \mathbb{R}^4_+$ *for every* $t > 0$.

Proof. Examining the local Lipschitz continuity of the coefficients in model (4.1), we observe that for any initial condition $(S(0), A(0), I(0), V(0)) \in \mathbb{R}^4$, there exists a positive constant π_e and a unique local solution $(S(t), A(t), I(t), V(t))$ defined on $[0, \pi_e]$, where π_e is referred to as the explosion time. To establish global existence, it suffices to prove that $\pi_e = \infty$.

Let $m_0 > 0$ be sufficiently large such that $S(0), A(0), I(0), V(0) \in \left[\frac{1}{m_0}, m_0\right]$. For each integer $m \geq m_0$, we define the stopping time

$$\pi_m = \inf\left\{t \in [0, \pi_e] : S(t) \notin \left(\frac{1}{m}, m\right), A(t) \notin \left(\frac{1}{m}, m\right), I(t) \notin \left(\frac{1}{m}, m\right), V(t) \notin \left(\frac{1}{m}, m\right)\right\}.$$

Clearly, $\{\pi_m\}$ is a non-decreasing sequence, and we define $\pi_\infty = \lim_{m\to\infty} \pi_m$. Then, it follows that $\pi_\infty \leq \pi_e$. If $\pi_\infty = \infty$, then necessarily $\pi_e = \infty$, implying that the solution is global, i.e., $(S(t), A(t), I(t), V(t)) \in \mathbb{R}^4$ for all $t > 0$. Conversely, if $\pi_\infty < \infty$, then there exist $T > 0$ and $\varepsilon \in (0, 1)$ such that $\mathbb{P}(\pi_\infty \leq T) \geq \varepsilon$. In particular, there exists some $m \geq m_0$ for which $\mathbb{P}(\pi_m \leq T) \geq \varepsilon$.

We define a C^4-function $W : \mathbb{R}^4_+ \to \mathbb{R}_+$, given by

$$W(S, A, I, V) = (S - a - a\ln\frac{S}{a}) + (A - 1 - \ln A) + (I - 1 - \ln I) + (V - 1 - \ln V),$$

where $a > 0$. Applying Itô's Lemma [36], we obtain

$$\begin{aligned} dW =& LWdt + \delta_1(S - a)dB_1(t) + \int_Y [q_1(y)S - a\ln(1 + q_1(y))]\tilde{N}(dt, dy) + \delta_2(A - 1)dB_2(t) \\ &+ \int_Y [q_2(y)A - \ln(1 + q_2(y))]\tilde{N}(dt, dy) + \delta_3(I - 1)dB_3(t) + \int_Y [q_3(y)I - \ln(1 + q_3(y))]\tilde{N}(dt, dy) \\ &+ \delta_4(V - 1)dB_4(t) + \int_Y [q_4(y)V - \ln(1 + q_4(y))]\tilde{N}(dt, dy), \end{aligned}$$

where

$$\begin{aligned} LW =& \int_Y \Big[aq_1(y) - a\ln(1 + q_1(y)) + q_2(y) - \ln(1 + q_2(y)) + q_3(y) - \ln(1 + q_3(y)) + q_4(y) \\ &- \ln(1 + q_4(y))\Big]\nu(dy) + \Lambda + 3\mu + (\mu + \varphi)a + \gamma_3 + \lambda + [(a + \rho)\beta - \mu]I - \mu S - \mu V \\ &- \mu R - \frac{a}{S}(1 - p)\Lambda - \frac{a_1 A}{(1 + b_1 A)S} - \frac{a_2 I}{(1 + b_2 I)S} - \frac{a}{S}\gamma_3\nu - \delta\beta S + \frac{a_1}{1 + b_1 A} - \beta S \\ &- \frac{\nu A}{I} + \frac{a_2}{1 + b_2 I} - \frac{p\Lambda}{V} - \frac{\varphi S}{V} - \frac{\gamma I}{R} + \frac{a\delta_1^2 + \delta_2^2 + \delta_3^2 + \delta_4^2}{2}. \end{aligned}$$

There is a constant N_0 for which

$$0 \leq \int_Y [q_i(y) - \ln(1 + q_i(y))]\, \nu(dy) \leq N_0, i = 1, 2, 3, 4.$$

Thus,

$$LW \leq \Lambda + 3\mu + (\mu + \varphi)a + \gamma_3 + \lambda + \frac{(a + \rho)\beta\Lambda}{\mu} + \frac{a\delta_1^2 + \delta_2^2 + \delta_3^2 + \delta_4^2}{2} + aN_0 + 3N_0 := K$$

and

$$
\begin{aligned}
dW \leqslant\ & Kdt + \delta_1(S-a)dB_1(t) + \int_Y [q_1(y)S - a\ln(1+q_1(y))]\tilde{N}(dt,dy) + \delta_2(A-1)dB_2(t) \\
& + \int_Y [q_2(y)A - \ln(1+q_2(y))]\tilde{N}(dt,dy) + \delta_3(I-1)dB_3(t) + \int_Y [q_3(y)I - \ln(1+q_3(y))]\tilde{N}(dt,dy) \\
& + \delta_4(V-1)dB_4(t) + \int_Y [q_4(y)V - \ln(1+q_4(y))]\tilde{N}(dt,dy).
\end{aligned} \tag{4.5}
$$

By combining both sides of the equation from 0 to $\pi_m \Lambda T$ and computing the average, we obtain

$$
0 \leq \mathbb{E}W(S(\pi_m\Lambda T), A(\pi_m\Lambda T), I(\pi_m\Lambda T), V(\pi_m\Lambda T)) \leq W(S(0), A(0), I(0), V(0)) + KT.
$$

Assuming $\Omega_m = \{\pi_m \leq T\}$, we have $\mathbb{P}(\Omega_m) \geq \varepsilon$. For any $\omega \in \Omega_m$, the quantities $S(\pi_m, \omega)$, $A(\pi_m, \omega)$, $I(\pi_m, \omega)$ and $V(\pi_m, \omega)$ will have at least one term equal to m or $\frac{1}{m}$. Consequently, we have

$$
\begin{aligned}
& W(S(\pi_m,\omega), A(\pi_m,\omega), I(\pi_m,\omega), V(\pi_m,\omega)) \\
& \geqslant \min\left\{m - 1 - \ln m, \frac{1}{m} - 1 + \ln m, m - a - a\ln\frac{m}{a}, \frac{1}{m} - a + a\ln\frac{m}{a}\right\}.
\end{aligned}
$$

Therefore, we obtain

$$
\begin{aligned}
& W(S(0), A(0), I(0), V(0)) + KT \geq \mathbb{E}\left[1_{\Omega_m} W(S(\omega), A(\omega), I(\omega), V(\omega))\right] \\
& \geq \varepsilon \min\left\{m - 1 - \ln m, \frac{1}{m} - 1 + \ln m, m - a - a\ln\frac{m}{a}, \frac{1}{m} - a + a\ln\frac{m}{a}\right\},
\end{aligned}
$$

where, 1_{Ω_m} represents the characteristic function of Ω_m. As $m \to \infty$, the limit of $W(S(0), A(0), I(0), V(0)) + KT$ tends to infinity, leading to a contradiction. Hence, it follows that $\pi_\infty = \infty$, implying that the model $(S(t), A(t), I(t), V(t))$ will not collapse within a finite time. The proof is complete. □

4.2. Eradication of infectious diseases

This section investigates the origins of disease eradication and its mathematical model. To facilitate subsequent derivations, we define the time-averaged value over the interval $[0, t]$ as

$$
\langle x(t)\rangle_t = \frac{1}{t}\int_0^t x(s)\,ds,
$$

where $\langle x(t)\rangle_t$ represents the dynamic variation of the variable $x(t)$ over the time period.

Next, we introduce the critical value $\tilde{R}_0$ to analyze the behavior of the probabilistic model (4.1), defined by

$$
\tilde{R}_0 = \frac{\beta\delta\Lambda + \mu\int_Y [\ln(1+q_2(y)) - q_2(y)]\,\nu(dy)}{\mu\left(\nu + \mu + \frac{\delta_2^2}{2}\right)}.
$$

This critical value plays a key role in examining the model's stability and the conditions under which disease eradication occurs. If $\tilde{R}_0 < 1$, the disease will tend to die out.

Theorem 4.2. *Let the initial values* $(S(0), A(0), I(0), V(0))$ *be non-negative real numbers in the positive quadrant* $\mathbb{R}^4_+$*, and let the sequence* $(S(t), A(t), I(t), V(t))$ *be a solution to the model described by Eq (4.1). Under the condition* $\tilde{R}_0 < 1$*, then,*

$$\begin{aligned}
\limsup_{t\to\infty} \frac{\ln A(t)}{t} &\leqslant \left(\nu + \mu + \frac{\delta_2^2}{2}\right)\left(\tilde{R}_0 - 1\right) \quad a.s.,\\
\lim_{t\to\infty}\langle S(t)\rangle_t &= \frac{\Lambda(\mu + \gamma_3 - p\mu)}{\mu(\mu + \varphi + \gamma_3)} \quad a.s.,\\
\lim_{t\to\infty}\langle V(t)\rangle_t &= \frac{\Lambda(p\mu + \varphi)}{\mu(\mu + \varphi + \gamma_3)} \quad a.s.,\\
\lim_{t\to\infty}\langle I(t)\rangle_t &= 0 \quad a.s..
\end{aligned}$$

Therefore, $I(t)$ *converges exponentially to zero almost surely, ensuring the eradication of the disease with probability 1.*

Proof. Sum all equations of model (4.1)

$$\begin{aligned}
d(S + A + I + V) =&[\Lambda - \mu(S + A + I + V)]dt + \delta_1 S(t)dB_1(t) + \delta_2 A(t)dB_2(t) + \delta_3 I(t)dB_3(t)\\
&+ \delta_4 V(t)dB_4(t) + \int_Y q_1(y)S(t)\tilde{N}(dt, dy) + \int q_2(y)A(t)\tilde{N}(dt, dy)\\
&+ \int_Y q_3(y)I(t)\tilde{N}(dt, dy) + \int_Y q_4(y)V(t)\tilde{N}(dt, dy).
\end{aligned} \tag{4.6}$$

Solving the Eq (4.6) over the interval $[0, t]$ gives

$$\langle S\rangle = \frac{\Lambda}{\mu} - \langle A\rangle - \langle I\rangle - \langle V\rangle + \varphi_1(t), \tag{4.7}$$

$$\langle S + V\rangle = \frac{\Lambda}{\mu} - \langle I\rangle - \langle A\rangle + \varphi_1(t), \tag{4.8}$$

where

$$\begin{aligned}
\varphi_1(t) = -\frac{1}{\mu}&\left(\frac{S(t) - S(0)}{t} + \frac{A(t) - A(0)}{t} + \frac{I(t) - I(0)}{t} + \frac{V(t) - V(0)}{t}\right) + \frac{1}{\mu}\Big[\delta_1 \frac{\int_0^t S(s)dB_1(s)}{t}\\
&+\delta_2 \frac{\int_0^t A(s)dB_2(s)}{t} + \delta_3 \frac{\int_0^t I(s)dB_3(s)}{t} + \delta_4 \frac{\int_0^t V(s)dB_4(s)}{t} + \frac{\int_0^t \int_Y q_1(y)S(s)\tilde{N}(ds, dy)}{t}\\
&+\frac{\int_0^t \int_Y q_2(y)A(s)\tilde{N}(ds, dy)}{t} + \frac{\int_0^t \int_Y q_3(y)I(s)\tilde{N}(ds, dy)}{t} + \frac{\int_0^t \int_Y q_4(y)V(s)\tilde{N}(ds, dy)}{t}\Big].
\end{aligned}$$

By using the method outlined in reference [39], we can obtain

$$\lim_{t\to\infty} \varphi_1(t) = 0. \tag{4.9}$$

Next, by applying the extended Itô's Lemma [40], we derive the following stochastic differential equation

$$
\begin{aligned}
d\ln A &= \left[\delta\beta S - \nu - \mu - \frac{a_1}{1+b_1A} - \frac{\delta_2^2}{2} + \int_Y (\ln(1+q_2(y)) - q_2(y))\,\nu(dy)\right]dt + \delta_2 dB_2(t) \\
&\quad + \int_Y \ln(1+q_2(y))\,\tilde{N}(dt,dy) \\
&\leq \left[\beta(S+V) - (\nu+\mu) - \frac{\delta_2^2}{2} + \int_Y (\ln(1+q_2(y)) - q_2(y))\,\nu(dy)\right]dt + \delta_2 dB_2(t) \\
&\quad + \int_Y \ln(1+q_2(y))\,\tilde{N}(dt,dy).
\end{aligned} \tag{4.10}
$$

Integrating Eq (4.10) over the interval $[0,t]$, dividing by t and applying (4.8), yields

$$
\frac{\ln A(t)}{t} \leqslant \beta\frac{\Lambda}{\mu} - (\nu+\mu) - \frac{\delta_2^2}{2} + \int_Y (\ln(1+q_2(y)) - q_2(y))\,\nu(dy) + \varphi_2(t), \tag{4.11}
$$

where

$$
\varphi_2(t) = \beta\varphi_1(t) + \frac{\int_0^t \delta_2 dB_2(s)}{t} + \frac{\int_0^t \int_Y \ln(1+q_2(y))\,\tilde{N}(ds,dy)}{t} + \frac{\ln A(0)}{t}.
$$

According to the Prime Number Theorem [41], we conclude $\lim_{t\to\infty}\varphi_2(t) = 0$.

If $\tilde{R}_0 < 1$, taking the limit of the inequality (4.11) yields

$$
\begin{aligned}
\limsup_{t\to\infty} \frac{\ln A(t)}{t} &\leqslant \left(\nu+\mu+\frac{\delta_2^2}{2}\right)\left(\frac{\beta\Lambda + \mu\int_Y (\ln(1+q_2(y)) - q_2(y))\,\nu(dy)}{\mu\left(\nu+\mu+\frac{\delta_2^2}{2}\right)} - 1\right) \\
&= \left(\nu+\mu+\frac{\delta_2^2}{2}\right)\left(\tilde{R}_0 - 1\right) < 0.
\end{aligned}
$$

By using the method in reference [42], we obtain

$$
\lim_{t\to\infty} A(t) = 0 \quad \text{a.s..} \tag{4.12}
$$

Next, by integrating the third equation of the model (4.1) over the interval $[0,t]$ and normalizing by t, we derive

$$
\begin{aligned}
\frac{I(t)-I(0)}{t} &= \beta\langle I\rangle\langle S\rangle + \nu\langle A\rangle - \mu\langle I\rangle - \langle\frac{a_2 I}{1+b_2 I}\rangle + \frac{\int_0^t \delta_3 I(s) dB_3(s)}{t} + \frac{\int_0^t\int_Y q_3(y) I(s)\tilde{N}(ds,dy)}{t} \\
&\geq \beta\langle I\rangle + \nu\langle A\rangle - \mu\langle I\rangle - a_2\langle I\rangle + \frac{\int_0^t \delta_3 I(s) dB_3(s)}{t} + \frac{\int_0^t\int_Y q_3(y) I(s)\tilde{N}(ds,dy)}{t},
\end{aligned}
$$

which implies

$$
\langle I\rangle \geqslant \frac{\nu}{\mu+a_2-\beta}\langle A\rangle + \frac{1}{\mu+a_2-\beta}\left[-\frac{I(t)-I(0)}{t} + \frac{\int_0^t \delta_3 I(s) dB_3(s)}{t} + \frac{\int_0^t\int_Y q_3(y) I(s)\tilde{N}(ds,dy)}{t}\right]. \tag{4.13}
$$

Combining this with equation (4.12), we conclude that

$$\lim_{t\to\infty}\langle I(t)\rangle = 0 \quad \text{a.s..} \tag{4.14}$$

Similarly, by integrating the right-hand side equation of model (4.1) over the interval $[0, t]$ and normalizing, we obtain

$$\frac{V(t)-V(0)}{t} = p\Lambda + \varphi\langle S\rangle - (\mu+\gamma_3)\langle V\rangle + \frac{\int_0^t \delta_4 V(s)dB_4(s)}{t} + \frac{\int_0^t\int_Y q_4(y)V(s)\tilde{N}(ds,dy)}{t}. \tag{4.15}$$

Combining with equation (4.7), we get

$$\begin{aligned}\frac{V(t)-V(0)}{t} &= p\Lambda + \varphi[\frac{\Lambda}{\mu} - \langle V\rangle - \langle A\rangle - \langle I\rangle + \varphi_1(t)] - (\mu+\gamma_3)\langle V\rangle + \frac{\int_0^t \delta_4 V(s)dB_4(s)}{t} \\ &\quad + \frac{\int_0^t\int_Y q_4(y)V(s)\tilde{N}(ds,dy)}{t},\end{aligned} \tag{4.16}$$

Thus,

$$\begin{aligned}\langle V\rangle &= \frac{\Lambda(p\mu+\varphi)}{\mu(\mu+\varphi+\gamma_3)} - \frac{\varphi}{\mu+\varphi+\gamma_3}[\langle I\rangle + \langle V\rangle - \varphi\varphi_1(t)] \\ &\quad + \frac{1}{\mu+\varphi+\gamma_3}\left[-\frac{V(t)-V(0)}{t} + \frac{\int_0^t \delta_4 V(s)dB_4(s)}{t} + \frac{\int_0^t\int_Y q_4(y)V(s)\tilde{N}(ds,dy)}{t}\right].\end{aligned} \tag{4.17}$$

Analogously, combining Eqs (4.9), (4.12) and (4.14), we deduce that

$$\lim_{t\to\infty}\langle V(t)\rangle_t = \frac{\Lambda(p\mu+\varphi)}{\mu(\mu+\varphi+\gamma_3)} \quad \text{a.s..} \tag{4.18}$$

Finally, it can be obtained by (4.7), (4.9), (4.12), (4.14) and (4.18) that

$$\lim_{t\to\infty}\langle S(t)\rangle_t = \frac{\Lambda(\mu+\gamma_3-p\mu)}{\mu(\mu+\varphi+\gamma_3)} \quad \text{a.s..}$$

□

4.3. Persistence of disease

This section examines the conditions under which disease transmission persists over time. To quantify this, we define $\tilde{R}_{jp}$ as

$$\tilde{R}_{jp} = \frac{\delta\beta\Lambda + \mu\int_Y [\ln(1+q_2(y)) - q_2(y)]\,\nu(dy)}{\mu\left(\nu+\mu+a_1+\frac{\delta_2^2}{2}\right)},$$

which represents the average transmission potential from infected individuals in population j to population p. This value serves as a measure of disease persistence between populations. If $\tilde{R}_{jp} > 1$, the disease can persist in the model, sustaining transmission over the long term.

Theorem 4.3. *Let the initial state variables* $(S(0), I(0), V(0), R(0)) \in \mathbb{R}^4_+$ *and let* $(S(t), I(t), V(t), R(t))$ *be the solution to model* (4.1)*. If* $\tilde{R}_{jp} > 1$*, then the following inequalities hold:*

$$\begin{aligned}
&\liminf_{t\to\infty}\langle S(t)\rangle_t \geqslant \frac{\mu\Lambda(1-p)}{\mu^2+\varphi\mu+\beta\Lambda} > 0 \quad a.s.,\\
&\liminf_{t\to\infty}\langle A(t)\rangle_t \geqslant \frac{(\mu+a_2-\beta)\left(\nu+\mu+a_1+\frac{\delta_2^2}{2}\right)}{\delta\beta(\mu+a_2+\nu-\beta)}\left[\tilde{R}_{jp}-1\right] > 0 \quad a.s.,\\
&\liminf_{t\to\infty}\langle I(t)\rangle_t \geqslant \frac{\nu\left(\nu+\mu+a_1+\frac{\delta_2^2}{2}\right)}{\delta\beta(\mu+a_2+\nu-\beta)}\left[\tilde{R}_{jp}-1\right] > 0 \quad a.s.,\\
&\liminf_{t\to\infty}\langle V(t)\rangle_t \geqslant \frac{p\Lambda(\mu^2+\varphi\mu+\beta\Lambda)+\varphi\mu\Lambda}{(\mu^2+\mu\varphi+\beta\Lambda)(\mu+\gamma_3)} > 0 \quad a.s..
\end{aligned}$$

Proof. From Eqs (4.8) and (4.13), we derive the inequality

$$\langle S+V\rangle \geqslant \frac{\Lambda}{\mu} - \left(1+\frac{\nu}{\mu+a_2-\beta}\right)\langle A\rangle + \varphi_3(t),$$

where

$$\varphi_3(t) = -\frac{1}{\mu+a_2-\beta}\Big[-\frac{I(t)-I(0)}{t} + \frac{\int_0^t \delta_3 I(s)dB_3(s)}{t} + \frac{\int_0^t\int_Y q_3(y)I(s)\tilde{N}(ds,dy)}{t}\Big] + \varphi_1(t).$$

From this, we conclude that $\lim_{t\to\infty}\varphi_3(t) = 0$, implying that $\varphi_3(t)$ vanishes as $t\to\infty$ and can thus be neglected. Next, combining Eq (4.10), we derive the stochastic differential equation for

$$\begin{aligned}
d\ln A &= \left[\delta\beta S - (\nu+\mu) - \frac{a_1}{1+b_1A} - \frac{\delta_2^2}{2} + \int_Y (\ln(1+q_2(y)) - q_2(y))\,\nu(dy)\right]dt + \delta_2 dB_2(t)\\
&\quad + \int_Y \ln(1+q_2(y))\,\tilde{N}(dt,dy)\\
&\geq \left[\delta\beta S - (\nu+\mu+a_1) - \frac{\delta_2^2}{2} + \int_Y (\ln(1+q_2(y)) - q_2(y))\,\nu(dy)\right]dt + \delta_2 dB_2(t)\\
&\quad + \int_Y \ln(1+q_2(y))\,\tilde{N}(dt,dy).
\end{aligned}$$

After appropriate transformations, this inequality becomes

$$\begin{aligned}
\frac{\ln A(t)}{t} &\geqslant \delta\beta\frac{\Lambda}{\mu} + \int_Y (\ln(1+q_2(y)) - q_2(y))\,\nu(dy) - (\nu+\mu+a_1) - \frac{\delta_2^2}{2} - \delta\beta\left(1+\frac{\nu}{\mu+a_2-\beta}\right)\langle A\rangle\\
&\quad + \frac{\int_0^t \delta_2 dB_2(s)}{t} + \frac{\int_0^t\int_Y \ln(1+q_2(y))\,\tilde{N}(ds,dy)}{t} + \varphi_4(t),
\end{aligned}$$

where

$$\varphi_4(t) = \delta\beta\varphi_3(t) + \frac{\ln A(0)}{t}.$$

We conclude that $\lim_{t\to\infty}\varphi_4(t)=0$, indicating that the influence of $\varphi_4(t)$ fades as t increases.

Assuming $\tilde{R}_{jp}>1$, applying the method from [43], we obtain

$$\begin{aligned}\liminf_{t\to\infty}\langle A\rangle &\geqslant \frac{(\mu+a_2-\beta)\left(\nu+\mu+a_1+\frac{\delta_2^2}{2}\right)}{\delta\beta(\mu+a_2+\nu-\beta)}\left[\frac{\delta\beta\Lambda+\mu\int_Y(\ln(1+q_2(y))-q_2(y))\,v(dy)}{\mu\left(\nu+\mu+a_1+\frac{\delta_2^2}{2}\right)}-1\right]\\ &=\frac{(\mu+a_2-\beta)\left(\nu+\mu+a_1+\frac{\delta_2^2}{2}\right)}{\delta\beta(\mu+a_2+\nu-\beta)}\left[\tilde{R}_{jp}-1\right]>0\quad\text{a.s..}\end{aligned}$$

From Eq (4.13), we have

$$\langle I\rangle\geqslant\frac{\nu}{\mu+a_2-\beta}\langle A\rangle+\varphi_5(t),$$

where

$$\varphi_5(t)=\frac{1}{\mu+a_2-\beta}\left[-\frac{I(t)-I(0)}{t}+\frac{\int_0^t\delta_3 I(s)dB_3(s)}{t}+\frac{\int_0^t\int_Y q_3(y)I(s)\tilde{N}(ds,dy)}{t}\right].$$

Similarly, we conclude $\lim_{t\to\infty}\varphi_5(t)=0$; hence, we deduce the following:

$$\liminf_{t\to\infty}\langle I\rangle\geqslant\frac{\nu\left(\nu+\mu+a_1+\frac{\delta_2^2}{2}\right)}{\delta\beta(\mu+a_2+\nu-\beta)}\left[\tilde{R}_{jp}-1\right]>0\quad\text{a.s..}$$

From the first equation in model (4.1), we can further deduce

$$dS\geqslant\left[(1-p)\Lambda-\left(\frac{\beta\Lambda}{\mu}+\mu+\varphi\right)S\right]dt+\delta_1 S\,dB_1(t)+\int_Y q_1(y)S\,\tilde{N}(dt,dy).\tag{4.19}$$

Integrating (4.19) over $[0,t]$ and averaging by t, get

$$\frac{S(t)-S(0)}{t}\geqslant(1-p)\Lambda-(\frac{\beta\Lambda}{\mu}+\mu+\varphi)\langle S\rangle+\frac{\int_0^t\delta_1 S(s)dB_1(s)}{t}+\frac{\int_0^t\int_Y q_1(y)S(s)\tilde{N}(ds,dy)}{t}.$$

Hence, we derive that

$$\liminf_{t\to\infty}\langle S\rangle\geqslant\frac{\mu\Lambda(1-p)}{\mu^2+\varphi\mu+\beta\Lambda}>0\quad\text{a.s..}$$

Finally, from the last equation in (4.1), we obtain

$$dV\geqslant[p\Lambda+\varphi S-(\mu+\gamma_3)V]\,dt+\delta_4 I dB_4(t)+\int_Y q_4(y)V\tilde{N}(dt,dy).\tag{4.20}$$

By a similar reasoning, integrating equation (4.20) over $[0,t]$ and averaging by t, we obtain

$$\frac{V(t)-V(0)}{t}\geqslant P\Lambda+\varphi\langle S\rangle-(\mu+\gamma_3)\langle V\rangle+\frac{\int_0^t\delta_4 V(s)dB_4(s)}{t}+\frac{\int_0^t\int_Y q_4(y)V(s)\tilde{N}(ds,dy)}{t},$$

Thus,

$$\liminf_{t\to\infty}\langle V\rangle\geqslant\frac{p\Lambda(\mu^2+\varphi\mu+\beta\Lambda)+\varphi\mu\Lambda}{(\mu^2+\mu\varphi+\beta\Lambda)(\mu+\gamma_3)}>0\quad\text{a.s..}$$

□

Based on the preceding analysis, model (4.1) possesses a unique global positive solution that is both non-negative and bounded. Specifically, when the extinction threshold $\tilde{R}_0 < 1$, the disease can be eradicated, whereas when the persistence threshold $\tilde{R}_{jp} > 1$, the epidemic transitions to an endemic state. These two thresholds quantify the interplay between control measures, transmission risks, and environmental disturbances, forming a decision threshold system that provides quantitative criteria for the classification of control strategies and parameter optimization. In Section 5, we will assess the model's practical applicability by fitting it to H1N1 and H3 influenza data. Additionally, simulations comparing deterministic models with stochastic trajectories, along with sensitivity analysis, will be conducted to investigate the impact of extreme disturbances, thereby facilitating the translation of theoretical findings into actionable insights for epidemic forecasting.

5. Numerical simulation

5.1. Real data example

Parameter estimation plays a pivotal role in validating the plausibility of influenza transmission models. Influenza dissemination encompasses intricate biological mechanisms, posing substantial challenges to precise mathematical modeling. To address this, PE leverages empirical epidemiological data to calibrate key parameters within plausible bounds, thereby enhancing the model's predictive accuracy and its capacity to capture transmission dynamics. Furthermore, by integrating metrics such as the basic reproduction number, accurate PE not only elucidates underlying transmission mechanisms but also furnishes a scientific foundation for optimizing intervention strategies.

To further investigate the dynamical properties of model (4.1), this section employs two sets of real-world influenza data from the United States in 2024 (comprising H1N1 and H3 positive cases) for parameter estimation, with the corresponding datasets illustrated in Figure 4[A,C] [44]. Utilizing model (2.1), we apply the least squares method to fit the parameters, where the fitted curves are depicted in Figure 4[B,D], and the resulting parameter estimates are summarized in Table 2.

To further investigate the capability of model (4.1) in characterizing the transmission dynamics of influenza, we adopted the parameters obtained from model fitting. Specifically, the white noise intensities were set as $\delta_1 = 0.2$, $\delta_2 = 0.22$, $\delta_3 = 0.35$, and $\delta_4 = 0.34$, while the Lévy jump intensities were set as $q_1 = 0.051$, $q_2 = 0.07$, $q_3 = 0.08$, and $q_4 = 0.05$. Under these parameter settings, the basic reproduction number was calculated as $\tilde{R}_0 = 0.205 < 1$. According to the theory of infectious disease dynamics, this indicates that the disease will eventually become extinct.

The results are presented in Figure 5[B], where the black dashed line represents the deterministic model, serving as a theoretical baseline in the absence of stochastic perturbations. However, this model fails to capture the complexity of real-world transmission processes. The red curve incorporates white noise factors, which lead to a better fit with the empirical data, reflecting the impact of persistent stochastic disturbances on the transmission dynamics. The blue curve includes both white noise and Lévy noise, the latter accounting for abrupt events, such as mass vaccination campaigns, stringent lockdowns, or sudden changes in control measures. The results show that the combined-noise model exhibits a significantly faster convergence to zero than the other two models, suggesting that the combined effects of white noise and Lévy noise accelerate the epidemic's decline and drive the number of infections toward zero more rapidly.

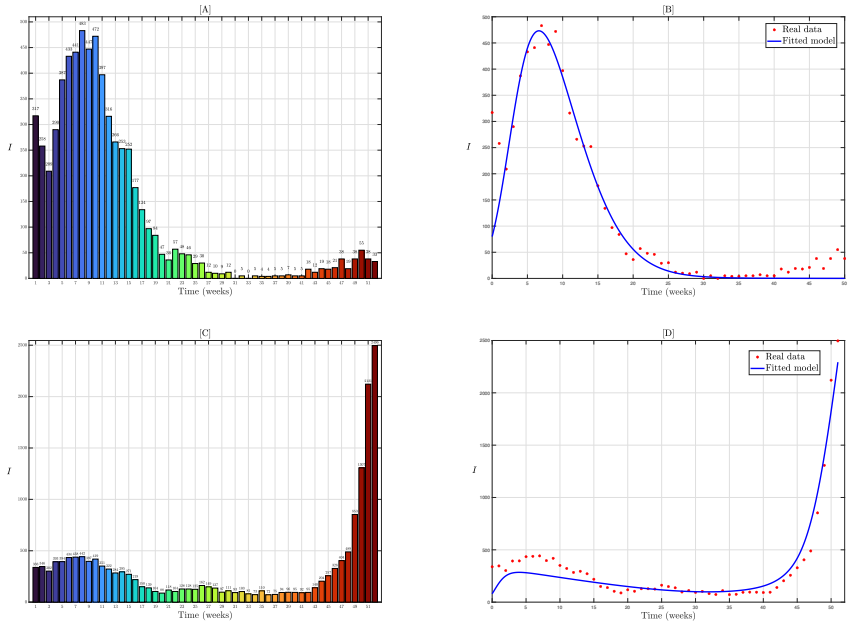

Figure 4. Real-world data and fitted curves for H1N1 and H3 positive influenza cases in the United States in 2024. [A] and [B] illustrate the weekly observed data and corresponding fitted curve for H1N1 positive cases, respectively; [C] and [D] illustrate the weekly observed data and corresponding fitted curve for H3 positive cases, respectively.

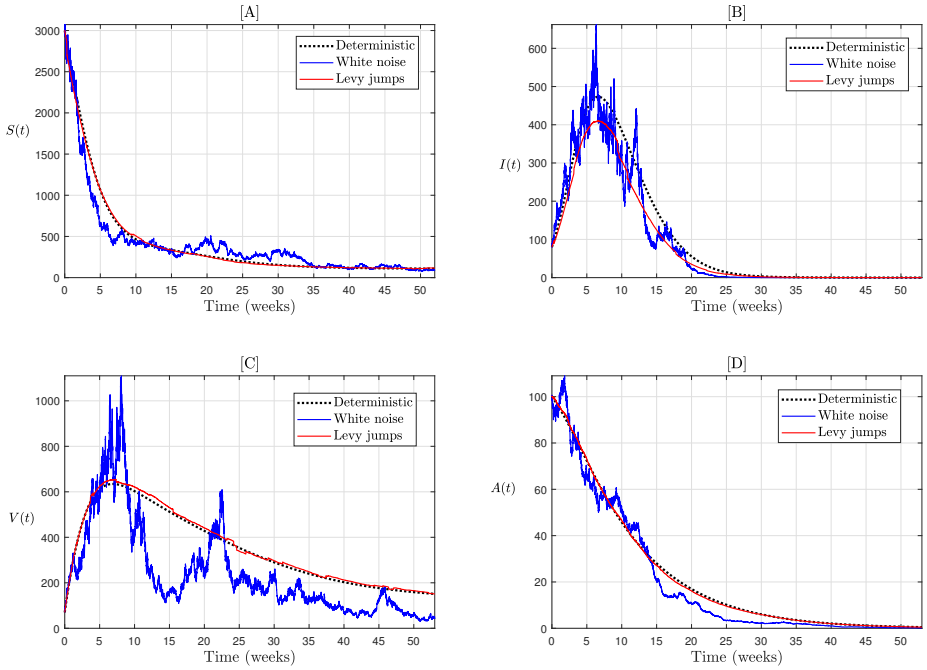

Figure 5. Deterministic and stochastic simulations of H1N1 outbreak and extinction dynamics.

5.2. *Sensitivity analysis*

According to the preceding analysis, $R_0 < 1$ implies that the influenza epidemic will eventually die out, whereas $R_0 > 1$ indicates that sustained transmission and possible epidemic escalation will occur. To systematically evaluate the relative contribution of each model parameter to R_0 and, consequently, to the transmission dynamics of influenza, we applied a normalized forward sensitivity analysis. This method quantifies the relative rate of change in the model output with respect to relative changes in individual parameters, thereby identifying those parameters exerting the greatest influence on disease spread and prioritizing them for accurate empirical estimation.

Mathematically, the normalized forward sensitivity index of R_0 with respect to a given parameter i is expressed as $\rho_i^{R_0} = \frac{\partial R_0}{\partial i} \times \frac{i}{R_0}$, where i denotes any parameter present in the analytical formulation of R_0 [22]. For example, for the transmission rate δ, we obtain $\rho_\delta^{R_0} = \frac{\partial R_0}{\partial \delta} \times \frac{\delta}{R_0} = 1$, indicating a directly proportional relationship between δ and R_0. Sensitivity indices for all other parameters were calculated using the same formulation, with results summarized in Table 3 and visualized in Figure 6.

Table 3. Parameter values and sensitivity indices comparison for R_0 calculation.

Parameter	Case 1		Case 2	
	Value	Sensitivity index	Value	Sensitivity index
β	0.000327	1.000000	0.000573	1.000000
Λ	20.00000	1.000000	200.729291	1.000000
δ	0.066475	1.000000	0.390928	1.000000
p	0.159279	-0.180806	0.220495	-0.000004
φ	0.074979	-0.453681	0.717417	-0.926573
ν	0.019223	-0.166439	0.163066	-0.243292
a_1	0.009475	-0.082037	0.507182	-0.756707
γ_3	0.003491	0.024532	0.056851	0.926561
μ	0.086798	-1.322375	0.000001	-0.999989

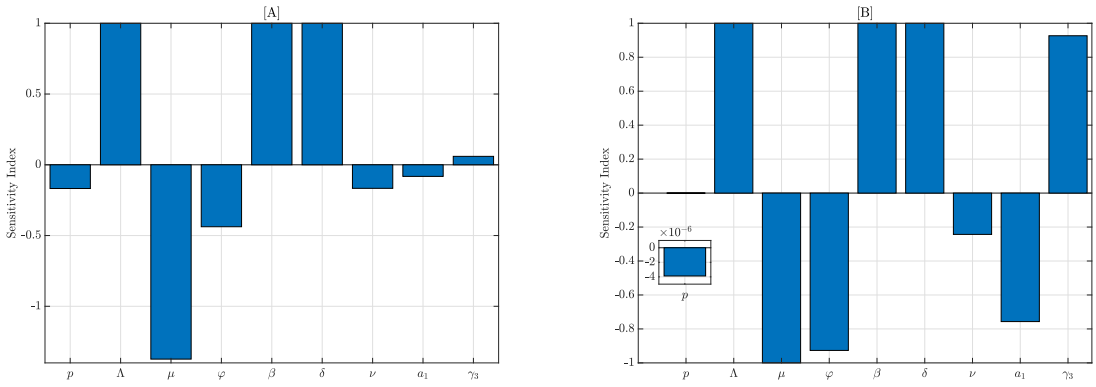

Figure 6. Sensitivity analysis of R_0 regarding the parameters of model (2.1).[A] parameters correspond to the fitted values in Table 3, Case 1, whereas [B] parameters correspond to the fitted values in Table 3, Case 2.

Sensitivity analysis indicates that the recruitment rate Λ, transmission rate β, and the relative transmissibility between infectious and vaccinated individuals δ exert significant positive effects on the basic reproduction number R_0. Specifically, β and δ enhance the efficiency of transmission between susceptible and infectious individuals, thereby accelerating disease spread, while Λ increases the pool of susceptible hosts, further facilitating epidemic propagation. In contrast, the natural mortality rate μ exhibits a negative effect on R_0, as it reduces the number of susceptible and infectious individuals, thus biologically suppressing the transmission of influenza.

Accordingly, the control of influenza should primarily focus on limiting population mobility (such as temporary closure of outbreak hotspots and restriction of external population inflow) and reducing effective contact rates (such as mask usage and avoidance of mass gatherings) to attenuate the influence of key driving parameters. Although other parameters exhibit comparatively lower sensitivity with respect to R_0, their epidemiological relevance remains non-negligible. For instance, enhancing the recovery rate of asymptomatic infectious individuals (a_1) or symptomatic infectious individuals (ν) can effectively shorten the infectious period and decrease the reservoir of infection, thereby functioning as complementary intervention strategies.

5.3. Stochastic persistence and extinction

In Theorems 4.2 and 4.3, stochastic extinction and persistence were characterized, establishing the critical conditions for epidemic dynamics under random environments and the role of noise in long-term behavior. To substantiate these results, Figures 7 and 8 compare the trajectories of infected individuals under different noise intensities, showing that fluctuations around the deterministic solution increase consistently with noise strength.

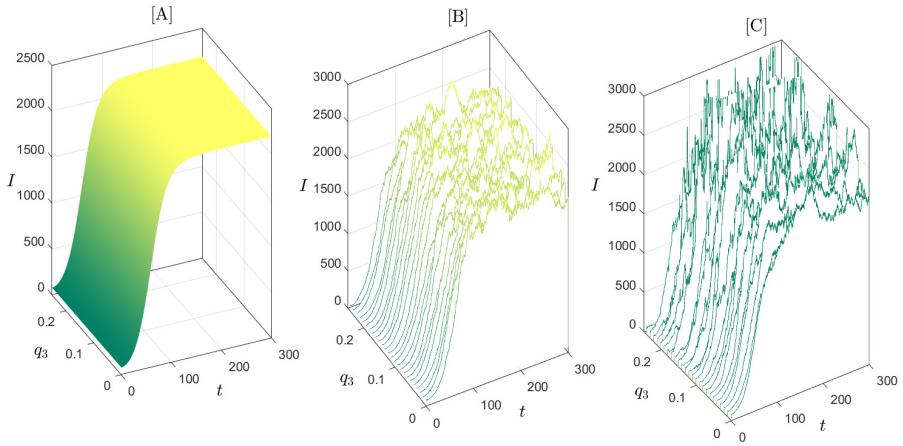

Figure 7. Endemic persistence scenario. Deterministic infected population ([A]), stochastic infected population with white noise ([B]), stochastic infected population with white noise and Lévy noise (C). The parameter as $\Lambda = 800, p = 0.2, \mu = 0.12, \varphi = 0.001, \beta = 0.00003, \delta = 0.8, \gamma_3 = 0.06, \nu = 0.016, a_1 = 0.006, a_2 = 0.0012, b_1 = 0.09, b_2 = 0.004, \delta_1 = 0.01, \delta_2 = 0.024, \delta_3 = 0.016, \delta_4 = 0.055, q_1 = 0.012, q_2 = 0.012, q_4 = 0.023$.

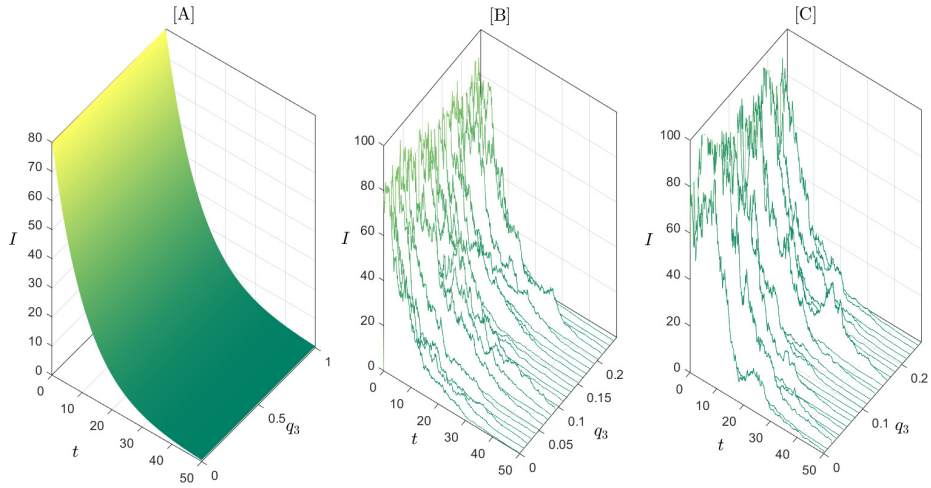

Figure 8. Endemic extinction scenario. Deterministic infected population ([A]), stochastic infected population with white noise ([B]), stochastic infected population with white noise and Lévy noise (C). The parameter as $\Lambda = 800, p = 0.1, \mu = 0.12, \varphi = 0.06, \beta = 0.000003, \delta = 0.00005, \gamma_3 = 0.06, \nu = 0.016, a_1 = 0.006, a_2 = 0.0012, b_1 = 0.09, b_2 = 0.004, \delta_1 = 0.052, \delta_2 = 0.09, \delta_3 = 0.16, \delta_4 = 0.08, q_1 = 0.1, q_2 = 0.17, q_4 = 0.05$.

Figure 7 demonstrates the epidemic outbreak regime with $\tilde{R}_0 = 1.1735 > 1$ and $\tilde{R}_{jp} = 1.1240 > 1$. The deterministic trajectory converges to the endemic equilibrium, confirming stable pathogen persistence in the absence of stochasticity. Incorporation of white noise induces limited oscillations around this equilibrium, indicating weak perturbations do not alter the endemic trend. Superimposing Lévy noise amplifies fluctuations with abrupt pulse-like deviations while preserving long-term endemic stability. Conversely, Figure 8 illustrates the disease extinction regime, achieved by reducing pathogen-vaccinee transmission ($\delta = 0.00005$), lowering baseline transmissibility ($\beta = 0.000003$), and enhancing interventions ($\varphi = 0.06$), resulting in $\tilde{R}_0 = 0.928 < 1$ and $\tilde{R}_{jp} = 0.089 < 1$. The deterministic solution exhibits monotonic decay to the disease-free equilibrium. White noise induces transient, damped oscillations around the extinction trajectory, while Lévy noise triggers occasional short-term rebounds without reversing the long-term extinction trend.

Accordingly, practical control efforts must account for both healthcare resource constraints and environmental stochasticity: resource saturation and sudden bottlenecks may delay case clearance, while environmental perturbations amplify uncertainty in transmission dynamics. Control strategies should encompass reducing transmission capacity (mask mandates and social distancing), dynamic containment measures, optimized resource allocation (expansion of ICU capacity, establishment of emergency reserves, and improved vaccine accessibility and coverage), and environmental risk management. Collectively, these measures can strengthen system resilience against Lévy-type shocks and environmental variability, ensuring that the reproduction number $R_0 < 1$ and sustaining long-term epidemic control.

6. Discussion

This study proposes an SAIV epidemic model (2.1) that incorporates limited healthcare resources and extends it into a stochastic SAIV model (4.1) driven by Lévy noise, considering environmental factors. The model focuses on analyzing the impact of healthcare resource constraints and environmental factors (such as seasonal variations and unexpected events) on influenza transmission. This provides a novel theoretical framework for a deeper understanding of influenza transmission dynamics and for optimizing prevention and control strategies.

First, the basic reproduction number R_0 was calculated using the next-generation matrix method, followed by a sensitivity analysis to quantify the impact of key factors on transmission dynamics. Furthermore, the study demonstrated the local and global asymptotic stability of the disease-free equilibrium. An innovative approach using nonlinear Volterra integral equations was employed to analyze the local stability of the disease equilibrium, providing a solid mathematical foundation for influenza epidemic prediction and control. Additionally, the study identified a transcritical bifurcation phenomenon (as shown in Figure 3), indicating that increasing vaccination rates, reducing vaccine failure rates, and implementing non-pharmaceutical interventions (such as mask-wearing and social distancing) can effectively reduce the risk of influenza transmission.

Furthermore, considering the complex impacts of environmental factors on influenza transmission–seasonal temperature affects both the influenza virus's activity and host immunity, while unexpected events may disrupt healthcare resources and thus influence viral spread. To address this, white noise and Lévy jump processes were introduced, leading to the development of a stochastic SAIV model (4.1). The existence, uniqueness, and non-negativity of the model's solution were proven. Additionally, the extinction threshold $\tilde{R}_0$ and persistence threshold $\tilde{R}_{jp}$ with Lévy jumps were defined, and the epidemic's persistence and extinction were analyzed using Lyapunov functions. The results indicated that when $\tilde{R}_0 < 1$, influenza tends to die out, whereas when $\tilde{R}_{jp} > 1$, influenza persists (see Figures 7 and 8). This analysis highlights the bidirectional regulatory effect of environmental noise on pathogen dynamics.

To validate the model's effectiveness, two sets of real influenza data are fitted using the least squares method. The model fitting results are satisfactory (as shown in Figure 4), demonstrating good predictive capability and practical value. Furthermore, to explore the impact of Lévy jump noise intensity on influenza transmission, we analyzed the variations in extinction and persistence under different noise intensities. The results showed that increasing noise intensity amplified random fluctuations, potentially accelerating disease outbreaks and prolonging transmission cycles, similar to the disruption caused by extreme environmental events on viral spread, which complicates influenza control efforts. Sensitivity analysis revealed that key parameters, such as the susceptible population influx rate Λ and the effective transmission contact rate β, significantly influence influenza transmission. Therefore, in control strategies, priority should be given to optimizing these key parameters, such as reducing population mobility to lower Λ, enhancing isolation to reduce β, and optimizing public health measures to lower the natural mortality rate d, in order to effectively control influenza transmission.

Finally, although this study comprehensively characterizes the effects of resource constraints and stochastic perturbations on influenza transmission, several limitations remain-most notably the omission of immunity delay, individual heterogeneity, and the oversimplification of spatial and

network interactions. Future work should incorporate these factors, integrate multi-source data with complex network models to improve predictive accuracy, and investigate adaptive intervention strategies within a model-based control framework.

Author contributions

Shunping Ouyang: Writing-review & editing, Software; Guoqin Chen and Yue Xia: Writing-original draft; Guoxing Shi: Idea, Methodology; Yanbin Feng: Formal analysis, Project Administration. Shunping Ouyang and Guoqin Chen contributed equally to this work and are considered co-first authors. Guoxing Shi and Yanbin Feng are the corresponding authors. All authors read and approved the final manuscript.

Use of AI tools declaration

The authors declare they have not used Artificial Intelligence (AI) tools in the creation of this article.

Acknowledgments

This work was supported by the Yunnan Province International Joint Laboratory for Intelligent Integration and Application of Ethnic Multilingualism (202403AP140014).

Data availability statement

The data used for numerical simulation in this study are sourced from references [44], and these data are publicly available, making them accessible for use.

Conflict of interest

Declare that there are no conflicts of interest regarding the publication of this paper.

References

1. M. Ali, F. Guma, A. Qazza, R. Saadeh, N. E. Alsubaie, M. Althubyani, et al., Stochastic modeling of influenza transmission: Insights into disease dynamics and epidemic management, *PDE Appl. Math.*, **11** (2024), 100886. https://doi.org/10.1016/j.padiff.2024.100886
2. X. Fu, Y. Zhou, J. Wu, X. Liu, C. Ding, C. Huang, et al., Clinical characteristics and outcomes during a severe influenza season in China during 2017–2018, *BMC Infect. Dis.*, **19** (2019), 668. https://doi.org/10.1186/s12879-019-4181-2
3. S. Kim, J. Lee, E. Jung, Mathematical model of transmission dynamics and optimal control strategies for 2009 A/H1N1 influenza in the Republic of Korea, *J. Theoret. Biol.*, **412** (2017), 74–85. https://doi.org/10.1016/j.jtbi.2016.09.025
4. A. Finckh, B. Gilbert, B. Hodkinson, S. C. Bae, R. Thomas, K. D. Deane, et al., Global epidemiology of rheumatoid arthritis, *Nat. Rev. Rheumatol.*, **18** (2022), 591–602. https://doi.org/10.1038/s41584-022-00827-y

5. A. El-shenawy, M. El-Gamel, D. Reda, Troesch's problem: A numerical study with cubic trigonometric B-spline method, *PDE Appl. Math.*, **10** (2024), 100694. https://doi.org/10.1016/j.padiff.2024.100694
6. S. Lee, M. Golinski, G. Chowell, Modeling optimal age-specific vaccination strategies against pandemic influenza, *Bull. Math. Biol.*, **74** (2012), 958–980. https://doi.org/10.1007/s11538-011-9704-y
7. S. Bugalia, J. P. Tripathi, H. Wang, Mathematical modeling of intervention and low medical resource availability with delays: Applications to COVID-19 outbreaks in Spain and Italy, *Math. Biosci. Eng.*, **18** (2021), 5865–5920. https://doi.org/10.3934/mbe.2021295
8. W. Qin, S. Zhang, Y. Yang, J. Zhang, A discrete SIR epidemic model incorporating media impact, resource limitaions and threshold switching strategies, *Infect. Dis. Model.*, **10** (2025), 1270–1290. https://doi.org/10.1016/j.idm.2025.07.006
9. B. Zhou, N. Shi, Analysis of a stochastic SEIS epidemic model motivated by Black–Karasinski process: Probability density function, *Chaos Solitons Fract.*, **189** (2024), 115713. https://doi.org/10.1016/j.chaos.2024.115713
10. Z. Cao, W. Feng, X. Wen, L. Zu, M. Cheng, Dynamics of a stochastic SIQR epidemic model with standard incidence, *Phys. A*, **527** (2019), 121180. https://doi.org/10.1016/j.physa.2019.121180
11. Y. Cai, Y. Kang, W. Wang, A stochastic SIRS epidemic model with nonlinear incidence rate, *Appl. Math. Comput.*, **305** (2017), 221–240. https://doi.org/10.1016/j.amc.2017.02.003
12. X. B. Zhang, X. H. Zhang, The threshold of a deterministic and a stochastic SIQS epidemic model with varying total population size, *Appl. Math. Model.*, **91** (2021), 749–767. https://doi.org/10.1016/j.apm.2020.09.050
13. D. Kiouach, Y. Sabbar, Developing new techniques for obtaining the threshold of a stochastic SIR epidemic model with 3-dimensional Lévy process, preprint paper, 2020. https://doi.org/10.48550/arXiv.2002.09022
14. S. Wang, G. Hu, T. Wei, L. Wang, Permanence of hybrid competitive Lotka-Volterra system with Lévy noise, *Phys. A*, **540** (2020), 123116. https://doi.org/10.1016/j.physa.2019.123116
15. J. Bao, C. Yuan, Stochastic population dynamics driven by Lévy noise, *J. Math. Anal. Appl.*, **391** (2012), 363–375. https://doi.org/10.1016/j.jmaa.2012.02.043
16. Q. Yang, X. Zhang, D. Jiang, Asymptotic behavior of a stochastic SIR model with general incidence rate and nonlinear Lévy jumps, *Nonlinear Dyn.*, **107** (2022), 2975–2993. https://doi.org/10.1007/s11071-021-07095-7
17. Y. Sabbar, A. Din, D. Kiouach, Influence of fractal–fractional differentiation and independent quadratic Lévy jumps on the dynamics of a general epidemic model with vaccination strategy, *Chaos Solitons Fract.*, **171** (2023), 113434. https://doi.org/10.1016/j.chaos.2023.113434
18. D. Kiouach, S. E. Azami El-idrissi, Y. Sabbar, The impact of Lévy noise on the threshold dynamics of a stochastic susceptible-vaccinated-infected-recovered epidemic model with general incidence functions, *Math. Meth. Appl. Sci.*, **47** (2024), 297–317. https://doi.org/10.1002/mma.9655
19. J. Djordevic, K. R. Dahl, Stochastic optimal control of pre-exposure prophylaxis for HIV infection for a jump model, *J. Math. Biol.*, **89** (2024), 55. https://doi.org/10.1007/s00285-024-02151-3

20. G. L. Anesi, Y. Lynch, L. Evans, A conceptual and adaptable approach to hospital preparedness for acute surge events due to emerging infectious diseases, *Crit. Care Explor.*, **2** (2020), e0110. https://doi.org/10.1097/CCE.0000000000000110

21. J. Andrade, B. Beishuizen, M. Stein, M. Connolly, J. Duggan, Preparing for pandemic response in the context of limited resources, *Syst. Dyn. Rev.*, **40** (2024), e1775. https://doi.org/10.1002/sdr.1775

22. W. Qin, X. Wu, Global analysis and optimal therapy in immunogenic tumors: A nonlinear state-dependent hybrid model with a dynamic threshold policy, *Nonlinear Dyn*, **113** (2025) 14013–14049. https://doi.org/10.1007/s11071-024-10847-w

23. X. Guan, F. Yang, Y. Cai, W. Wang, Global stability of an influenza A model with vaccination, *Appl. Math. Lett.*, **134** (2022), 108322. https://doi.org/10.1016/j.aml.2022.108322

24. J. Zhang, J. Jia, X. Song, Analysis of an SEIR epidemic model with saturated incidence and saturated treatment function, *Sci. World J.*, **2014** (2014), 910421. https://doi.org/10.1155/2014/910421

25. J. K. Ghosh, U. Ghosh, M. H. A. Biswas, S. Sarkar, Qualitative analysis and optimal control strategy of an SIR model with saturated incidence and treatment, *Differ. Equ. Dyn. Sys.*, **31** (2023), 53–67. https://doi.org/10.1007/s12591-019-00486-8

26. F. Brauer, C. Castillo-Chavez, Z. Feng, *Mathematical models in epidemiology*, New York: Springer, 2019.

27. S. Boulaaras, Z. U. Rehman, F. A. Abdullah, R. Jan, M. Abdalla, A. Jan, Coronavirus dynamics, infections and preventive interventions using fractional-calculus analysis, *AIMS Math*, **8** (2023), 8680–8701. http://dx.doi.org/10.3934/math.2023436

28. H. W. Hethcote, D. W. Tudor, Integral equation models for endemic infectious diseases, *J. Math. Biol.*, **9** (1980), 37–47. https://doi.org/10.1007/BF00276034

29. T. Vu, S. Farish, M. Jenkins, H. Kelly, A meta-analysis of effectiveness of influenza vaccine in persons aged 65 years and over living in the community, *Vaccine*, **20** (2002), 1831–1836. https://doi.org/10.1016/S0264-410X(02)00041-5

30. A. Alkhazzan, J. Wang, Y. Nie, H. Khan, J. Alzabut, A novel SIRS epidemic model for two diseases incorporating treatment functions, media coverage, and three types of noise, *Chaos Solitons Fract.*, **181** (2024), 114631. https://doi.org/10.1016/j.chaos.2024.114631

31. J. Guckenheimer, P. Holmes, *Nonlinear oscillations, dynamical systems, and bifurcations of vector fields*, Berlin: Springer, 2013.

32. P. Sandhu, A. B. Shah, F. B. Ahmad, J. Kerr, H. B. Demeke, E. Graeden, et al., Emergency department and intensive care unit overcrowding and ventilator shortages in US hospitals during the COVID-19 pandemic, 2020-2021, *Public Health Rep.*, **137** (2022), 796–802. https://doi.org/10.1177/00333549221091781

33. A. M. Salman, I. Ahmed, M. H. Mohd, M. S. Jamiluddin, Scenario analysis of COVID-19 transmission dynamics in Malaysia with the possibility of reinfection and limited medical resources scenarios, *Comput. Biol. Med.*, **133** (2021), 104372. https://doi.org/10.1177/00333549221091781

34. J. Maurya, K. B. Blyuss, A. K. Misra, Modeling the impact of hospital beds and vaccination on the dynamics of an infectious disease, *Math. Biosci.*, **368** (2024), 109133. https://doi.org/10.1016/j.mbs.2023.109133
35. X. Zou, K Wang, Numerical simulations and modeling for stochastic biological systems with jumps, *Commun. Nonlinear Sci. Numer. Simul.*, **19** (2014), 1557–1568. https://doi.org/10.1016/j.cnsns.2013.09.010
36. X. Mao, *Stochastic differential equations and applications*, Amsterdam: Elsevier, 2007.
37. A. El Koufi, A. Bennar, N. Yousfi, Dynamics behaviors of a hybrid switching epidemic model with levy noise, *Appl. Math.*, **15** (2021), 131–142. http://doi.org/10.18576/amis/150204
38. M. El Fatini, R. Taki, A. Tridane, Threshold behaviour of a stochastic epidemic model with two-dimensional noises, *Phys. A*, **524** (2019), 776–786. https://doi.org/10.1016/j.physa.2019.04.224
39. X. Jing, G. Liu, Z. Jin, Stochastic dynamics of an SEIR epidemic model on heterogeneous networks: A case of COVID-19, *Int. J. Biomath.*, **8** (2025), 2550007. https://doi.org/10.1142/S179352452550007X
40. A. Adiga, D. Dubhashi, B. Lewis, M. Marathe, S. Venkatramanan, A. Vullikanti, Mathematical models for covid-19 pandemic: A comparative analysis, *J. Indian Inst. Sci.*, **100** (2020), 793–807.
41. Y. Zhou, W. Zhang, Threshold of a stochastic SIR epidemic model with Lévy jumps, *Phys. A*, **446** (2016), 204–216. https://doi.org/10.1016/j.physa.2015.11.023
42. Y. Sabbar, A. Khan, A. Din, D. Kiouach, S. P. Rajasekar, Determining the global threshold of an epidemic model with general interference function and high-order perturbation, *AIMS Math.*, **7** (2022), 19865–19890. http://dx.doi.org/10.3934/math.20221088
43. K. Fan, Y. Zhang, S. Gao, S. Chen, A delayed vaccinated epidemic model with nonlinear incidence rate and Lévy jumps, *Phys. A*, **544** (2020), 123379. https://doi.org/10.1016/j.physa.2019.123379
44. *Number of specimens testing positive for influenza in the United States in 2024, by week and subtype/lineage*, Statista, 2025. Available online: `https://www.statista.com/statistics/1122427/influenza-cases-number-us-by-subtype-week/`.

AIMS Press